THE STRUCTURE OF SELF-ASSEMBLED MONOLAYERS OF ALKYLSILOXANES ON SILICON: A COMPARISON OF RESULTS FROM ELLIPSOMETRY AND LOW-ANGLE X-RAY REFLECTIVITY

S. R. Wasserman and G. M. Whitesides*
Department of Chemistry
and I. M. Tidswell, B. M. Ocko, and Peter S. Pershan*
Division of Applied Sciences and Department of Physics
Harvard University
Cambridge MA 02138

and J. D. Axe
Department of Physics
Brookhaven National Laboratory
Upton NY 11973

Technical Report No. 15 (May 1989)

Interim Technical Report

(Accepted for publication in J. Am. Chem. Soc.

PREPARED FOR DEFENSE ADVANCED RESEARCH PROJECTS AGENCY
1400 Wilson Boulevard
Arlington VA 22209

DEPARTMENT OF THE NAVY
Office of Naval Research, Code 1130P
800 North Quincy Street
Arlington VA 22217-5000

ARPA Order No.: NR 356-856
Contract No.: N00014-85-K-0898
Effective Date: 85 September 01
Expiration Date: 89 May 31

Principal Investigator: George M. Whitesides
(617) 495-9430

REPRODUCED AT GOVERNMENT EXPENSE

SECURITY CLASSIFICATION OF THIS PAGE

REPORT DOCUMENTATION PAGE

1a. REPORT SECURITY CLASSIFICATION Unclassified	1b. RESTRICTIVE MARKINGS
2a. SECURITY CLASSIFICATION AUTHORITY	3. DISTRIBUTION / AVAILABILITY OF REPORT Approved for public release; distribution unlimited
2b. DECLASSIFICATION / DOWNGRADING SCHEDULE	
4. PERFORMING ORGANIZATION REPORT NUMBER(S) Technical Report # 15	5. MONITORING ORGANIZATION REPORT NUMBER(S)
6a. NAME OF PERFORMING ORGANIZATION Harvard University 6b. OFFICE SYMBOL (If applicable)	7a. NAME OF MONITORING ORGANIZATION Office of Naval Research
6c. ADDRESS (City, State, and ZIP Code) Office of Sponsored Research Holyoke Center, Fourth Floor Cambridge MA 02138-4993	7b. ADDRESS (City, State, and ZIP Code) Code 1130P 800 North Quincy Street Arlington VA 22217-5000
8a. NAME OF FUNDING / SPONSORING ORGANIZATION ONR/DARPA 8b. OFFICE SYMBOL (If applicable)	9. PROCUREMENT INSTRUMENT IDENTIFICATION NUMBER
8c. ADDRESS (City, State, and ZIP Code) 800 North Quincy Street Arlington VA 22217-5000	10 SOURCE OF FUNDING NUMBERS PROGRAM ELEMENT NO. 85-K-0398 / PROJECT NO. NR 356-856 / TASK NO. / WORK UNIT ACCESSION NO

11. TITLE (Include Security Classification) "The Structure of Self-Assembled Monolayers of Alkylsiloxanes on Silicon: A Comparison of Results from Ellipsometry and Low-Angle X-Ray Reflectivity"

12. PERSONAL AUTHOR(S) Wasserman, S. R.; Whitesides, G. M.; Tidswell, I. M.; Ocko, B. M., et al.

13a. TYPE OF REPORT	13b. TIME COVERED	14. DATE OF REPORT (Year, Month, Day)	15. PAGE COUNT
Interim	FROM ____ TO ____	May 1989	

16. SUPPLEMENTARY NOTATION

17. COSATI CODES		
FIELD	GROUP	SUB-GROUP

18. SUBJECT TERMS (Continue on reverse if necessary and identify by block number)
self-assembly, monolayer, alkylsiloxane, ellipsometry, X-ray reflectivity, thickness, alkyl compounds, siloxanes, silanes

19. ABSTRACT (Continue on reverse if necessary and identify by block number)

The thicknesses of alkylsiloxane monolayers on silicon/silicon dioxide substrates have been measured using ellipsometry and low angle X-ray reflection. Thicknesses measured by the two methods differ by 2.2 Å (rms) for alkyl chains of 10 - 18 carbon atoms and have a maximum difference of 4.2 Å. Ellipsometry systematically yields a larger →

(over)

20. DISTRIBUTION / AVAILABILITY OF ABSTRACT	21. ABSTRACT SECURITY CLASSIFICATION
☒ UNCLASSIFIED/UNLIMITED ☐ SAME AS RPT ☐ DTIC USERS	
22a. NAME OF RESPONSIBLE INDIVIDUAL Dr. Joanne Milliken	22b. TELEPHONE (Include Area Code) / 22c. OFFICE SYMBOL

DD FORM 1473, 84 MAR 83 APR edition may be used until exhausted. All other editions are obsolete

SECURITY CLASSIFICATION OF THIS PAGE

19. ABSTRACT (Cont'd)

cont'd → thickness. This discrepancy may result from differences between the two techniques in their sensitivity to the structure of the interface between silicon dioxide and the alkylsiloxane monolayer. The X-ray reflectivity measurements provide evidence that these organic monolayers do not build up as island structures and demonstrate that the approximate area projected by each alkyl group in the plane of the monolayer is approx 20 ± 4 for- Å^2. Preliminary studies indicate that the use of this technique to follow changes in the structure of a monolayer as a result of transformations in its constitution are complicated by damage (often oxidation) to the monolayer that is induced by X-ray radiation.

← Keywords:

REVISED: # JA882727C-30-9-269

The Structure of Self-Assembled Monolayers of Alkylsiloxanes on Silicon: A Comparison of Results from Ellipsometry and Low-Angle X-Ray Reflectivity

Stephen R. Wasserman and George M. Whitesides*
Department of Chemistry, Harvard University, Cambridge, MA 02138

Ian M. Tidswell, Ben M. Ocko, and Peter S. Pershan*
Division of Applied Sciences and Department of Physics, Harvard University, Cambridge, MA 02138

John D. Axe
Department of Physics, Brookhaven National Laboratory, Upton, NY 11973

Abstract

The thicknesses of C10-C18 alkylsiloxane monolayers on silicon-silicon dioxide substrates have been measured using ellipsometry and low angle X-ray reflection. Although, for any given sample, thicknesses measured by the two methods agree to within experimental error, ellipsometric measurements are systematically larger by approximately 2 Å. This difference may result from variations in the sensitivity of the two techniques to the structure of the interface between silicon dioxide and the alkylsiloxane monolayer. The X-ray reflectivity measurements provide evidence that these

organic monolayers do not build up as island structures and demonstrate that the approximate area projected by each alkyl group in the plane of the monolayer is ~ 21 ± 3 $Å^2$. Preliminary studies indicate that this technique can be used to follow the changes in the structure of a monolayer which result from chemical transformations. The influence of damage that is induced by X-ray radiation on these measurements is discussed.

Introduction

This paper describes the use of ellipsometry and low-angle X-ray reflectivity to characterize monolayers prepared by reaction of alkyltrichlorosilanes with the surface silanol groups of silicon bearing a hydrated native oxide. Our primary objective was to compare estimates of the thicknesses of these films obtained using these two techniques. Ellipsometry has been employed extensively for the measurement of the thicknesses of thin organic films.[1-5] X-ray reflectivity is just beginning to be used for this purpose.[6-11] Agreement between ellipsometry and X-ray reflectivity would help to validate both techniques. A secondary objective was to examine the structural order of these self-assembled alkylsiloxane monolayers. As part of this work we have attempted to generate monolayers that have a variation in electron density along the normal to the substrate surface. The intensity of the X-rays reflected from such samples is sensitive to this type of change in electron density.[6,12] The determination of the electron distribution in films ostensibly having variations in electron density along the z-axis would provide one direct measure of order in these systems.

Previous studies have attempted to verify the accuracy of ellipsometry in determining the thicknesses of organic monolayers. For Langmuir-Blodgett monolayers estimates of thickness by ellipsometry, isotopic labelling,[13,14] and surface pressures[15] are in agreement. These experiments

depended, however, on comparisons of complete and partial monolayers and demonstrated only that the thickness of a monolayer as measured by ellipsometry correlates with the number of molecules per unit area in that monolayer and their length. We have reached a similar conclusion when correlating the ellipsometric thicknesses of monolayers prepared from a homologous series of alkyltrichlorosilanes with the relative intensities of carbon and silicon observed in X-ray photoelectron spectroscopy (XPS).[16] This conclusion has also been reached in related experiments that utilized monolayers of alkyl thiols adsorbed on gold films.[17]

Against the background of these earlier studies, we had two reasons to conduct a comparison of results from ellipsometry and X-ray reflection. First, these previous studies did not directly measure the thickness of the monolayers. Second, they examined Langmuir-Blodgett, rather than self-assembled, monolayers.

The self-assembled monolayers used in this work were prepared by placing a silicon-silicon dioxide (Si/SiO_2) substrate in a solution containing an alkyltrichlorosilane ($RSiCl_3$).[18] The Si-Cl bonds react with silanol groups[19] and adsorbed water[20] present on the surface of the silicon dioxide, and form a network of Si-O-Si bonds of undefined structure.[21] The resulting monolayers are bound covalently to the substrate and are stable. X-ray photoelectron spectroscopy (XPS) reveals that no chlorine remains in them.[16] The density of surface silanol groups on the native

oxide is only ~ 1 per 20 Å^2.[22,23] This density is approximately equal to the surface density of R groups within the monolayer (see below). The remaining Si-Cl bonds of the $RSiCl_3$ groups apparently react with water[24] and form -Si-O-Si- and/or -Si-OH moieties.

Ellipsometry and low-angle X-ray reflection are both optical techniques based on the reflection of light from interfaces. Although these two techniques are described using the same theoretical treatment -- Fresnel's equations for the reflection of light[25] -- they measure different properties of the light reflected from an interface. In addition, the wavelengths of the light used here in ellipsometry (λ = 6328 Å) and X-ray reflection ($\lambda \approx 1.5 - 1.7$ Å) differed by more than a factor of 10^3. The two techniques are also sensitive to different facets of interfacial structure.

Results

Preparation of Monolayers. We prepared alkylsiloxane monolayers on silicon-silicon dioxide (Si/SiO_2) substrates by reaction with alkyltrichlorosilanes using techniques similar to those described previously.[16,18,26] Because the measurement of X-ray reflection requires large, flat samples, the silicon substrates for these studies were significantly larger (2.5 x 7.5 cm) and, in general, thicker (0.125 in.) than those used previously.[27] Some samples were, however, prepared on thin (0.015 in.) substrates.[28] We

examined monolayers prepared from saturated alkyltrichlorosilanes ($Cl_3Si(CH_2)_nCH_3$, n = 9,11,14,15,17), from 16-heptadecenyltrichlorosilane (HTS, $Cl_3Si(CH_2)_{15}CH=CH_2$), and from a fluorinated silane ($Cl_3Si(CH_2)_2(CF_2)_7CF_3$).

Ellipsometry. The theory of ellipsometry has been discussed in detail by others.[1,29] Here we summarize certain important details and assumptions of the method.

Ellipsometry analyzes the reflection of elliptically polarized light from an interface separating two media with different indices of refraction. This elliptically polarized light can be represented as the sum of two components, one in the plane of incidence of the light (p polarization), the other perpendicular to this plane (s polarization). Upon reflection the amplitude and phase of each of these components is altered, resulting in a change in the overall polarization and amplitude of the light wave. These changes in amplitude and phase are represented by the Fresnel reflection coefficients for the p and s polarizations, r_p and r_s. Ellipsometry measures the ratio of these coefficients, ρ. The standard relationships between ρ and the measured analyzer (A) and polarizer (P) angles are summarized in equations 1-3.[1,29]

$$\rho = \frac{r_p}{r_s} = \tan \Psi \exp (i\Delta) \qquad (1)$$

$$\Psi = A \qquad (2)$$

$$\Delta = 2P + \pi/2 \qquad (3)$$

The angle Ψ represents the ratio of the changes in amplitude for the s and p polarizations of light upon reflection from an interface. The angle Δ is the difference in the phase shifts that are experienced by each polarization upon reflection.

In order to use ellipsometry to determine the thickness of a monolayer supported on a substrate, one must compare data obtained from the monolayer-substrate system with those from the uncoated substrate.[30] This comparison is straightforward, but differences between the substrate in coated and uncoated form may skew the ellipsometric results. Clean silicon-silicon dioxide has a high surface free energy and, therefore, a high affinity for both water and organic contaminants. Organic monolayers terminating in methyl and vinyl groups have low interfacial free energies and resist contamination.[31] If contamination of the bare Si/SiO_2 substrate were significant, we would expect that the thicknesses of the monolayers as measured by ellipsometry would be too small. We have found that the thicknesses of these n-alkylsiloxane monolayers correspond very closely to those which we expect for a trans-extended chain oriented perpendicular to the surface:[16] that is, to the largest plausible thickness. A trans-extended chain is in agreement with infrared measurements of chain geometry.[32] We conclude, based on these two lines of evidence, that contamination does not appear to affect the ellipsometric results in these systems.[33]

The conventional interpretation of the ellipsometric data is based on a model consisting of parallel interfaces separating air, the alkylsiloxane monolayer, and the substrate (Figure 1). The effectively infinitely thick substrate has a refractive index n_2, the monolayer has a uniform refractive index n_1, and the ambient atmosphere has refractive index n_0 (which is assumed to be 1). Since the silicon substrates have a native surface oxide layer,[34,35] a three-layer model might, in principle, provide a more accurate representation of the structure of the monolayer. In practice we have used a two-layer model and have measured a single effective refractive index for the substrate that combines contributions from the bulk silicon and the surface oxide.[36] Although we assume that the two interfaces, monolayer-substrate and air-monolayer, are perfectly smooth, theoretical and experimental studies suggest that, for ellipsometry, roughness has little effect on the measured thickness of the monolayer.[37-39]

Ellipsometry can, in principle, determine both the thickness and the refractive index of a monolayer. For the very thin (< 50 Å) films examined here, it is not, however, possible to determine both of these quantities simultaneously.[40] We must, therefore, assume a value for one of them before calculating the other. We have chosen to model the monolayer as a transparent medium with a refractive index of 1.45;[41] other investigators have used a refractive index of 1.50 for organic monolayers.[5] Our value is

Figure 1. Two-layer model used for ellipsometry. The silicon substrate has refractive index n_2, the monolayer has refractive index n_1, and the ambient air has refractive index n_0. The interfaces between each layer are assumed to be perfectly sharp. For the alkylsiloxane monolayers on silicon n_2 is ~ 3.8, n_1 is ~ 1.45, and n_0 is assumed to be 1. The incident angle of the laser light, ϕ_0, is 70°. The angles of refraction, $\phi_1 \approx 40°$ and $\phi_2 \approx 15°$, are given by Snell's law ($n_1 \sin\phi_1 = n_2 \sin\phi_2$).

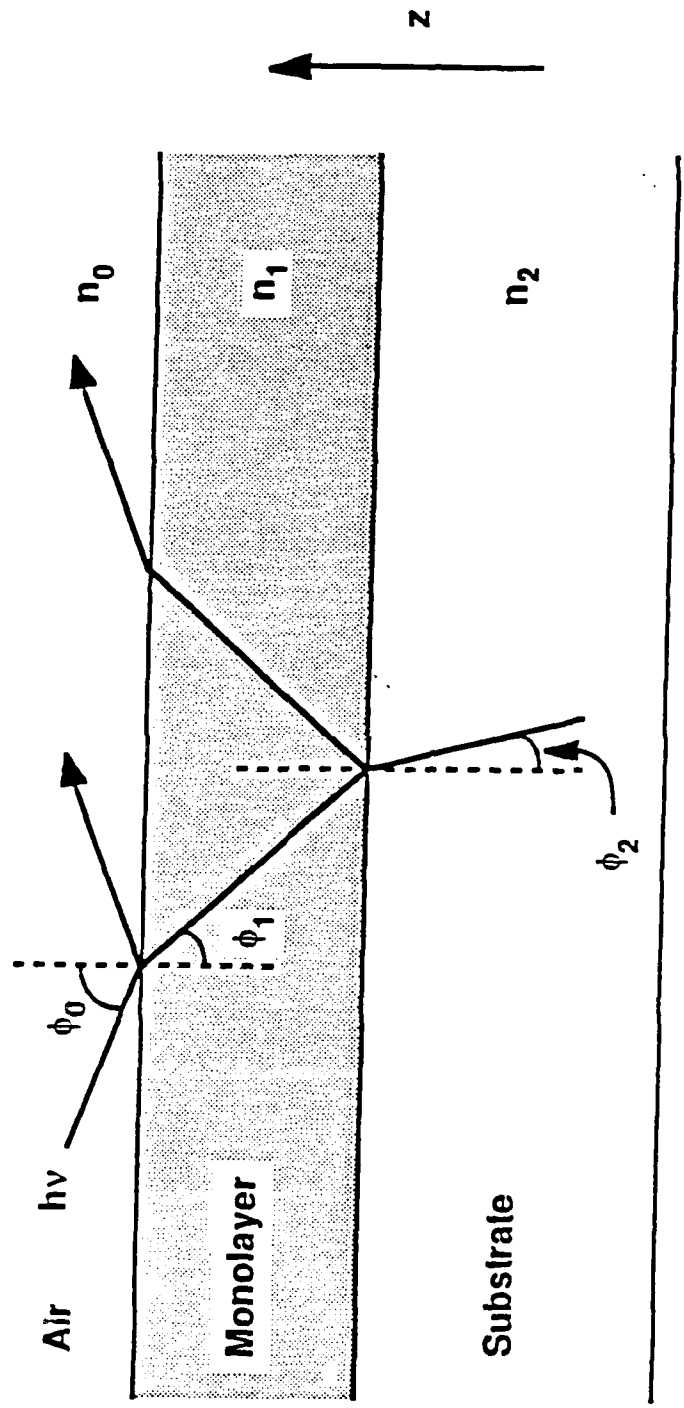
z
n_0
n_1
n_2
ϕ_0
ϕ_1
ϕ_2
hν
Air
Monolayer
Substrate

approximately that of pure liquid and crystalline paraffins (1.42-1.44)[42] but is lower than that of high density polyethylenes (1.49-1.55).[43] While our choice of refractive index is somewhat arbitrary, the X-ray reflectivity measurements (see below) suggest that the electron density in these monolayers is similar to that of bulk paraffins.[44-47] For the monolayers examined here, an increase of 0.05 in the assumed value of the index of refraction of the monolayer would decrease its calculated thickness by ~ 0.8 - 1.3 Å.[48]

For ellipsometry we used a helium-neon laser (λ = 6328 Å) as the light source. Other wavelengths within the visible region would provide similar results.[5] The method has an accuracy on the order of ± 2 Å.

Low-Angle X-Ray Reflectivity. The reflection of X-rays from surfaces[6] has been used to characterize the structural properties of several systems, including liquids[49-51] and liquid crystals.[52-54] We and others have already described the theory of this technique[55] and its use for the characterization of the structure of monolayers prepared from alkyltrichlorosilanes.[8,27] We will only summarize certain features of the method.

Low-angle X-ray reflectivity measures the intensity, R, of X-rays that are reflected from a surface as a function of the angle, θ, between the incoming X-ray beam and the sample. In general the variation of this intensity with θ is given by Fresnel's laws. The intensity also varies as a result of the change in the difference in phase between X-rays reflected

from the air-monolayer and monolayer-substrate interfaces. R is related to $\langle d\rho_{el}/dz \rangle$,[56] the average derivative of the electron density along the normal (z) axis of the substrate, by equation 4. Here hq_z (eq 5) is the change in momentum

$$R = R_F \left| \rho_\infty^{-1} \int_{-\infty}^{\infty} \langle d\rho_{el}/dz \rangle \exp(iq_z z)\, dz \right|^2 \qquad (4)$$

$$q_z = 4\pi\lambda^{-1}\sin\theta \qquad (5)$$

experienced by the X-ray photons during the reflection process,[57] while ρ_∞ is the electron density of the bulk substrate. R_F is the Fresnel reflectivity, the intensity of X-rays reflected from a bare substrate whose boundary with a vacuum is sharp and perfectly smooth. If the refractive index of the substrate is known, the form of R_F is determined solely by the Fresnel reflection coefficients. This index of refraction is calculated from the critical angle, θ_c, for total reflection of the X-rays.[55] The refractive index in the X-ray region is a linear function of the electron density, ρ_{el}.[58] The change in electron density $d\rho_{el}/dz$ is therefore a direct measure of dn/dz.

Equation 4 describes the pattern of interference that results from the reflection of X-rays from an arbitrary electron distribution, $\rho_{el}(z)$. In the case of two sharp interfaces separated by some distance, eq 4 reduces to the familiar interference condition for reflection from parallel

surfaces.[59,60] Since the measured interference pattern depends on the actual distance separating the two interfaces in our monolayer system, this method, unlike ellipsometry, directly measures the thickness of the monolayer.

Our experiments utilized two monochromatized sources of X-rays: a rotating anode (λ = 1.54 Å) and the National Synchrotron Light Source (NSLS, λ = 1.71 Å). We present the data obtained from these two sources as a function of q_z because the interference pattern is invariant in q_z, regardless of the wavelength of radiation used. We will also usually present our data in the form R/R_F. Since for a single sharp interface $R = R_F$,[59] $R/R_F = 1$ for all q_z. Any divergence of ρ_{el} from that characterizing a single ideal interface is, therefore, readily apparent as deviations in R/R_F from a horizontal line.

The interpretation of the observed interference pattern (Figure 2 shows typical data) requires fitting it to a structural model of the monolayer that incorporates changes in the electron density along the surface normal ($d\rho_{el}/dz$). We have analyzed our data using a treatment described in detail elsewhere[61] and summarized graphically in Figure 3. This two-layer model is the simplest plausible model for the description of the alkylsiloxane monolayers, but it is not an exact representation of the monolayer-substrate system. The presence of the surface oxide on the silicon substrate might suggest the use of a three-layer model. The electron densities of amorphous silicas and bulk silicon are, however,

Figure 2. Intensity, R, of X-rays reflected from alkylsiloxane monolayers on silicon-silicon dioxide substrates as a function of q_z, the momentum change of the photon upon reflection. The monolayers were prepared from alkyltrichlorosilanes, $Cl_3Si(CH_2)_nCH_3$. The top spectrum is for bare Si/SiO_2. Each spectrum is offset by 10^3 from the one above it. The solid line is the calculated Fresnel reflectivity, R_F, for a perfectly smooth silicon substrate.

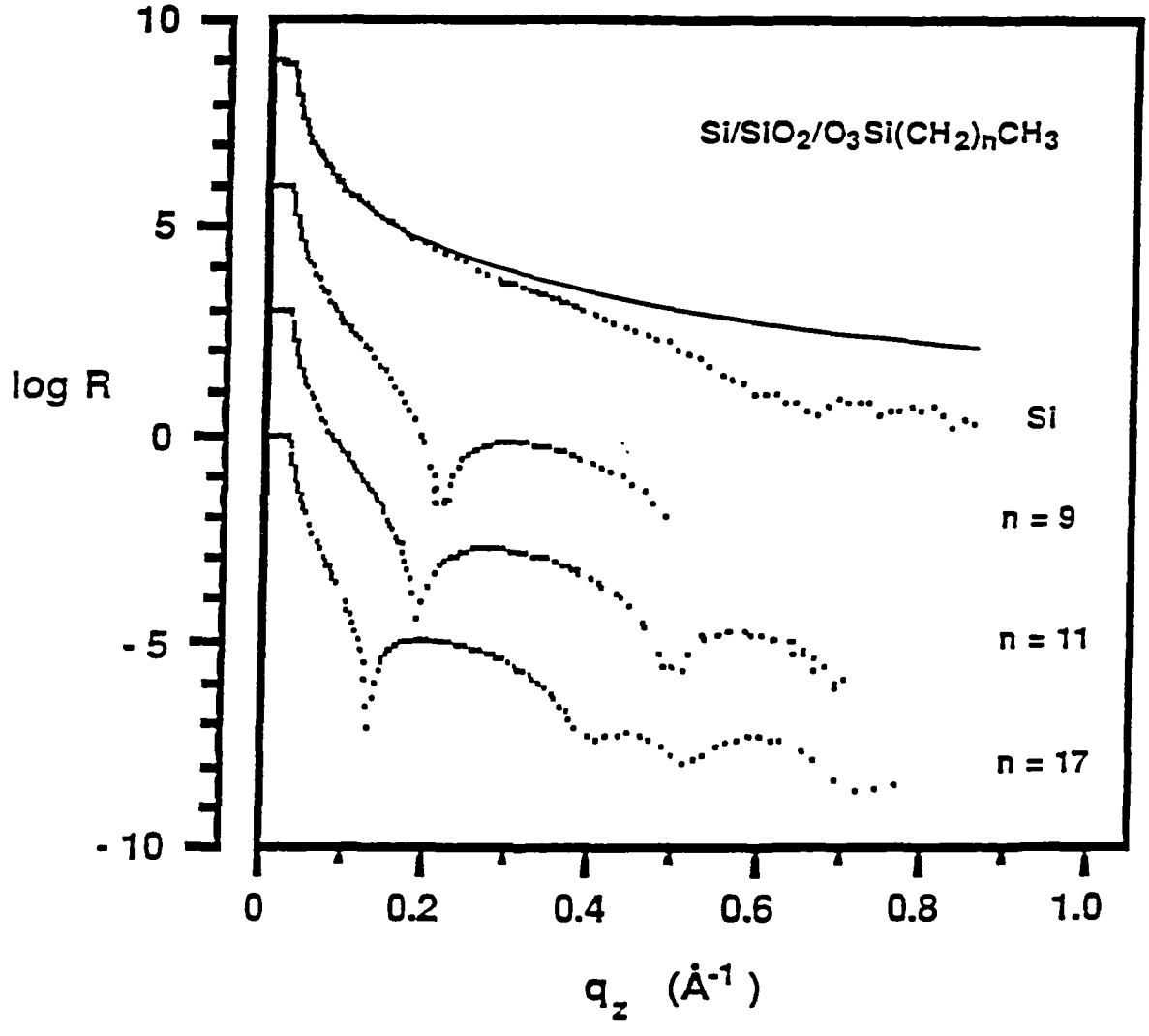
10
5
0
- 5
- 10
log R
Si/SiO2/O3Si(CH2)nCH3
Si
n = 9
n = 11
n = 17
0
0.2
0.4
0.6
0.8
1.0
qz (Å-1)

Figure 3. Models for ρ_{el}, the electron density, and $d\rho_{el}/dz$, the change in electron density along the normal perpendicular to the plane of the monolayer, used to analyze the measured X-ray reflectivity of alkylsiloxane monolayers on Si/SiO_2 substrates. The air-monolayer and monolayer-substrate interfaces are represented in $d\rho_{el}/dz$ by Gaussian functions, $A_1\exp(z^2/2\sigma_1^2)$ and $A_2\exp((z-d)^2/2\sigma_2^2)$. The parameter d, the separation between the centers of these functions, represents the distance between the air-monolayer and monolayer-substrate interfaces. This distance is the thickness of the monolayer. A_1, A_2, σ_1, and σ_2 are the heights and widths of the Gaussian functions. The parameters $\delta\rho_1$ and $\delta\rho_2$ are the changes in electron density across each interface and are proportional to $A_1\sigma_1$ and $A_2\sigma_2$. The electron density decreases from substrate to monolayer to air. The index of refraction for X-rays is a linear function of the electron density.

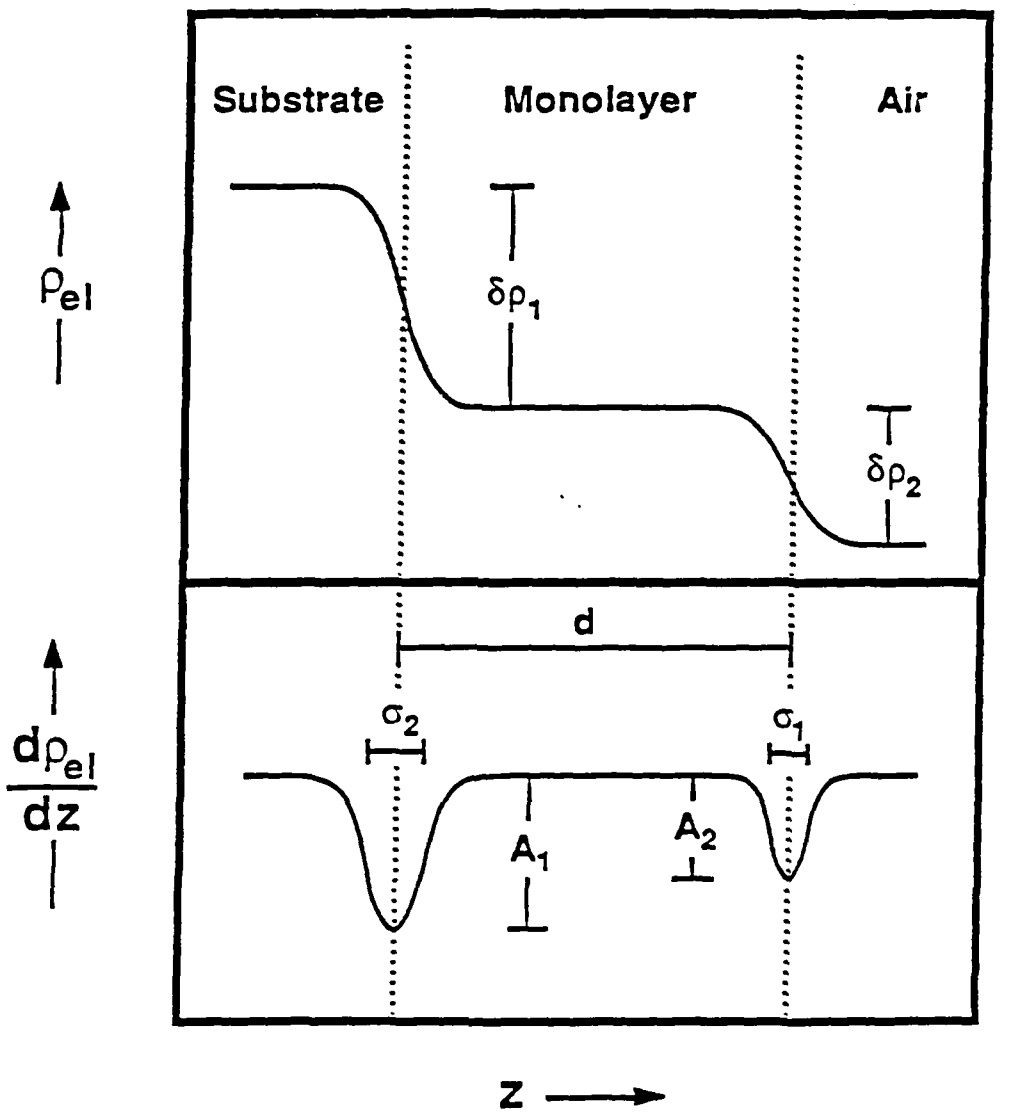
Substrate
Monolayer
Air
ρ_{el}
$\delta\rho_1$
$\delta\rho_2$
d
$\frac{d\rho_{el}}{dz}$
σ_2
σ_1
A_1
A_2
z

very similar.[62] To the X-rays the silicon and silicon dioxide therefore appear, to a first approximation, as a single material with no separating interface.[63] In this paper we will use the two-layer model to determine the thicknesses of the alkylsiloxane monolayers. In a separate paper[27] we discuss the uncertainties associated with this model and demonstrate how the thickness of the monolayer depends slightly on the model used.

Our model describes $d\rho_{el}/dz$ for each interface as a Gaussian function, $Aexp(z^2/2\sigma^2)$. The model contains five parameters: the thickness of the monolayer, d (actually the distance between the centers of the substrate-monolayer and monolayer-air interfaces), the height of each Gaussian, A_1 and A_2, and their widths, σ_1 and σ_2.[64] The σ parameters represent the roughnesses and intrinsic widths of both interfaces. The changes in electron density across each interface, $\delta\rho_1$ and $\delta\rho_2$, are proportional to $A_1\sigma_1$ and $A_2\sigma_2$ respectively. The positions of the minima in the X-ray profile are determined almost entirely by d. The thickness of the monolayer can therefore be determined to an accuracy of ~ 1 Å. The amplitudes of the minima, as well as the general shape of the profile of the scattered X-rays, reflect the combined effects of A_1, A_2, σ_1, and σ_2. Because these parameters are coupled, obtaining reliable values for them is technically complex.[27]

X-ray reflectivity does not utilize comparisons between the bare substrate and the coated sample to measure the

thickness of the monolayer. Differences in susceptibility to contamination between the substrate and the monolayer would therefore have no effect on the measured length of the monolayer. Adsorption of impurities on the monolayer would, however, cause an increase in its apparent thickness. During the several hours required for the accumulation of the X-ray data, we have observed the buildup of a contaminant layer on the higher-energy Si/SiO_2 surface.[33] We have not detected such contamination when a monolayer is present.

X-ray Damage. While ellipsometry is a non-destructive technique, exposure of an organic monolayer to synchrotron radiation results in some degradation of the sample. The experiments reported here were conducted under air rather than in vacuum or under an inert gas. We found that, upon removal from the X-ray beam, the contact angle of water on a methyl-terminated monolayer had decreased by 25 - 40° from $\theta_a^{H_2O} = 112°$ to $\theta_a^{H_2O} = 72 - 88°$.[65] This lowered contact angle appeared only on the central portion of the sample: that is, the area that had been exposed to the greatest flux of X-rays. The edge of this sample, which had had little or no exposure to X-rays, exhibited unchanged wettability ($\theta_a^{H_2O} = 112°$). Ellipsometry failed to discern any significant difference between the damaged and pristine regions.

Figure 4 presents XPS spectra of the C 1s peaks from the center and edge regions of a monolayer prepared from dodecyltrichlorosilane ($Cl_3Si(CH_2)_{11}CH_3$). The damaged area,

Figure 4. XPS spectra of a monolayer prepared from $Cl_3Si(CH_2)_{11}CH_3$ showing radiation damage caused by exposure to X-rays from a synchrotron source: survey spectra (left) and high resolution spectra of the C 1s region (right). A) Edge of sample unexposed to X-rays. The contact angle in this region was $\theta_a^{H_2O} = 112°$. The contact angle and XPS spectra of this area were indistinguishable from those of monolayers that had not been exposed to any X-ray radiation. No carbon atoms in oxidized environments are observed. B) Central area of sample exposed to the greatest flux of X-rays. The contact angle in this region was $\theta_a^{H_2O} = 82°$. The high-resolution C 1s spectrum exhibits a tail to higher binding energy, indicating the presence of oxidized carbon species.

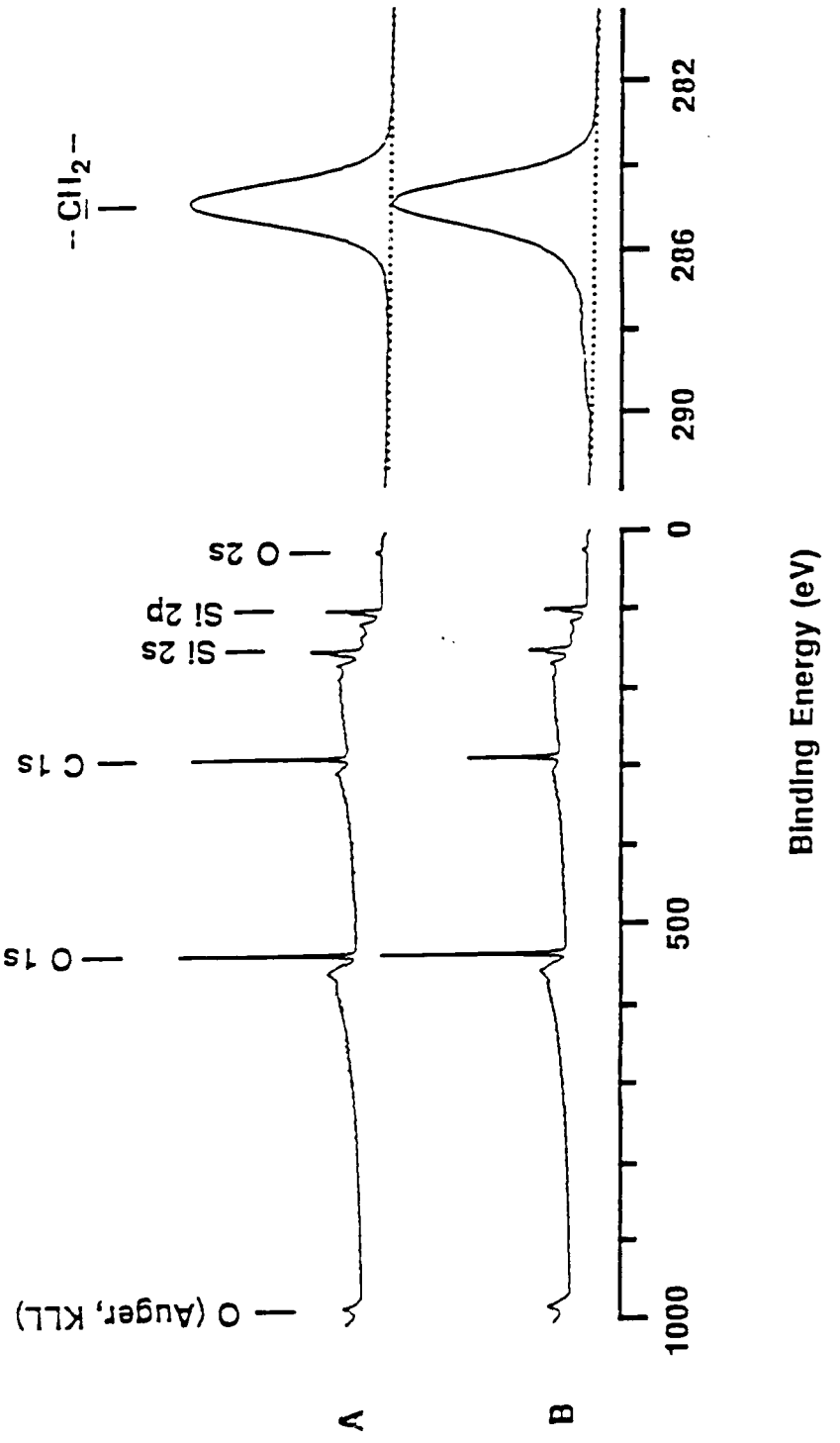
A
B
O (Auger, KLL)
O 1s
C 1s
Si 2s
Si 2p
O 2s
1000
500
0
290
286
282
Binding Energy (eV)
C 1s
CH2

which had θ_a^{H2O} = 82°, shows a tailing to higher binding energy that is not present in the areas unexposed to the radiation. We suspect that these changes in θ_a^{H2O} and the XPS spectra reflect oxidation of the monolayer to polar, oxygen-containing functionalities (alcohols, ketones, carboxylic acids, hydroperoxides, and/or others).[66] We could not detect these new oxygen signals directly by XPS against the large background signal from the oxygen atoms in the surface silicon oxide. This type of damage apparently requires exposure to intense X-rays. Samples that had only been exposed to radiation from a rotating anode source, whose flux was approximately 0.1% of that of the synchrotron, exhibited no change in θ_a^{H2O} or in XPS spectra.[67]

Although the damage to the monolayer was clearly measurable, we do not, for two reasons, believe that it had a significant effect on the value of the thickness measured for the monolayer. First, samples examined on both the rotating anode and the synchrotron exhibited similar reflectivities. Second, the information of primary importance in determining the thickness of the monolayer using the two-layer model -- the position of the first intensity minimum in the reflected X-rays -- was derived after relatively brief exposure to the X-rays.[68]

Thickness of Alkylsiloxane Monolayers on Silicon. We applied both X-ray reflectivity and ellipsometry to a set of alkylsiloxane monolayers (Figure 5). For fifteen samples and six chain lengths, the agreement between the two

Figure 5. Comparison of the thicknesses of alkylsiloxane monolayers as measured by ellipsometry and X-ray reflectivity. The solid circles (●) are the thicknesses of complete monolayers; the open circles (○) are the thicknesses of partial monolayers. The solid line is that expected if the two techniques yield the same thickness. The dotted line is offset by 1.4 Å and is that expected if only ellipsometry includes the silicon atom of the alkylsilane in the measured thickness (see text).

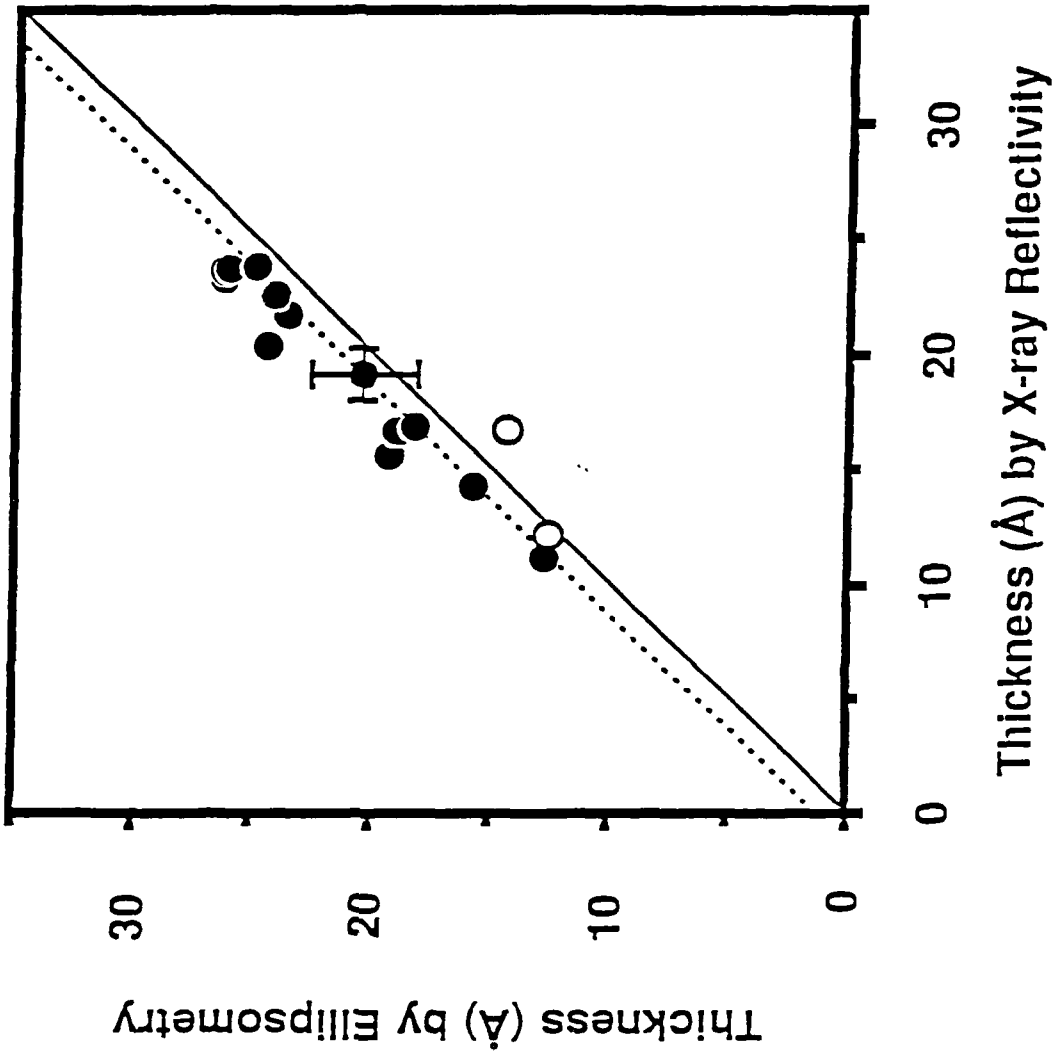
Thickness (Å) by Ellipsometry
0
10
20
30
Thickness (Å) by X-ray Reflectivity
0
10
20
30

techniques is good. The maximum deviation between the thicknesses estimated using the two methods is 4.2 Å; the average difference is 2.2 Å (rms). This accuracy is equivalent to an error of ~ 10% in the measurement of the thickness of a C_{18} monolayer.

Ellipsometry systematically gives larger values of thickness. This difference could result from the use of too low a value for the refractive index of the monolayer. We would, however, require $n \simeq 1.55$ in order to obtain values for the width of the monolayers from ellipsometry commensurate with those from the X-ray measurements. While such a high refractive index is found for crystalline polyethylene,[43] it seems unreasonable for a hydrocarbon monolayer that contains methyl groups.

We believe that the discrepancy between the thicknesses inferred from ellipsometric and X-ray measurements is, at least in part, the result of a subtle difference in the two methods. The ellipsometric thicknesses are based on differences in measurements of the bare substrate and the substrate with an attached alkylsiloxane monolayer. The refractive index of SiO_2 is 1.46[69] and the contribution of an $-O_3SiCH_2-$ moiety to the index of refraction of the monolayer is probably very close to that of the alkyl chain, R. Thus, the thickness measured by ellipsometry <u>includes</u> the silicon atom of the alkylsiloxane group. In the X-ray experiment the measured thickness corresponds to the distance separating interfaces between media of different electron densities.

Since the electron density of the silicon atom in the $RSiO_3$- group that attaches the monolayer to the substrate is effectively indistinguishable from that of the oxide layer on the substrate, the silicon atom of the alkylsilane group appears to the X-rays to be part of the substrate, not of the hydrocarbon monolayer. In short, ellipsometry measures the thickness of a $-Si(CH_2)_nCH_3$ monolayer; X-rays, of a $-(CH_2)_nCH_3$ monolayer. This explanation suggests that thicknesses estimated by ellipsometry should be ~ 1.4 Å longer than those estimated by X-ray reflectivity.[70] These considerations cannot account for all the observed difference between the two sets of measurements. The remaining difference (~ 0.7 Å) probably reflects minor deficiencies in the models used in analyzing the ellipsometric and X-ray data.

Projected Area of Alkylsiloxane Groups in the Plane of the Monolayer. The data from low-angle X-ray scattering provides a semi-quantitative estimate of the in-plane area of each alkylsiloxane group in these monolayers. The critical angle for total reflection from the substrate, θ_c, is related to the electron density of the silicon substrate ρ_{elSi} (eq 6).[55] The observed critical angle,

$$\theta_c^2 = \frac{\lambda^2 \rho_{el} r_o}{\pi} \qquad r_o = 2.818 \times 10^{-5} \text{ Å} \qquad (6)$$

$\theta_c = 0.225 \pm 0.007°$ for X-rays having wavelength $\lambda = 1.54$ Å,[71] corresponds to an electron density of 0.72 ±

0.05 $Å^{-3}$. The expected value for silicon, 0.70 $Å^{-3}$, is in good agreement with this number. The fitting of the profile of scattered X-rays to the model of $\langle d\rho_{el}/dz \rangle$ for the covered substrate gives an estimate of the electron density of the monolayer, $\rho_{el_{mono}}$, relative to that of the substrate. For the n-alkane monolayers studied here, we estimate, using a three-layer model, that $\rho_{el_{mono}}/\rho_{el_{Si}} = 0.43 \pm 0.05$.[27,72] The area per alkylsiloxane group, A, can then be calculated from this estimate of the electron density of the monolayer, the thickness of the monolayer, d, and the number of electrons, N_e, in the alkyl group of each alkylsiloxane moiety (eq 7).[73] Our calculated value for A is 21 ±

$$A = \frac{N_e}{d\rho_{el}} \qquad (7)$$

3 $Å^2$ per RSi- group.[74] An alternative analysis, based on monolayers that had been prepared from dodecyl- and octadecyltrichlorosilane, yields an area of 22.5 ± 2.5 Å.[27] These areas are similar to that found for close-packed Langmuir-Blodgett monolayers of long-chain alcohols (20.5-22 $Å^2$)[75] and to the cross-sectional area per molecule within crystals of long chain paraffins (20.5 $Å^2$).[44,45] Other studies have concluded that these self-assembled structures are themselves at or near a close-packed arrangement.[18] Our results are consistent with this conclusion.

Structure of Incompletely Formed Monolayers. We would like to be able to assess the process by which

alkyltrichlorosilanes adsorb and bind to a silicon substrate. While we cannot, with our current level of technical sophistication, directly analyze this process, we can determine certain features of the structure of incompletely formed (partial) monolayers. The analysis of these structures may, in turn, shed light on how complete monolayers are formed.

We generated partial monolayers by removing the substrates from the solutions containing the alkyltrichlorosilanes before the monolayers had formed completely. We hypothesized two extreme possibilities for the structure of such monolayers (Figure 6). A complete monolayer is characterized by a length, d, and a refractive index, n_1. In one possible structure for an incomplete monolayer, the alkyl chains would be uniformly distributed over the substrate, but would be disordered and have a liquid-like structure. In this "uniform" case the monolayer would have a refractive index similar to that of the complete monolayer, but its thickness would be less. In the second structure, the monolayer would consist of islands of alkylsiloxane groups having local structure similar to that of the complete monolayer. In this "island" model, the thickness would be the same as that of the complete monolayer, but the average refractive index of the monolayer would be lower. We cannot, using ellipsometry, distinguish

Figure 6. Models for the structure of incomplete monolayers. A complete monolayer has a thickness, d, and an index of refraction, n_1. In the uniform model the partial monolayer has a length less than d and an index of refraction approximately equal to n_1. In the island model the incomplete monolayer has a thickness, d, but the index of refraction is less than n_1.

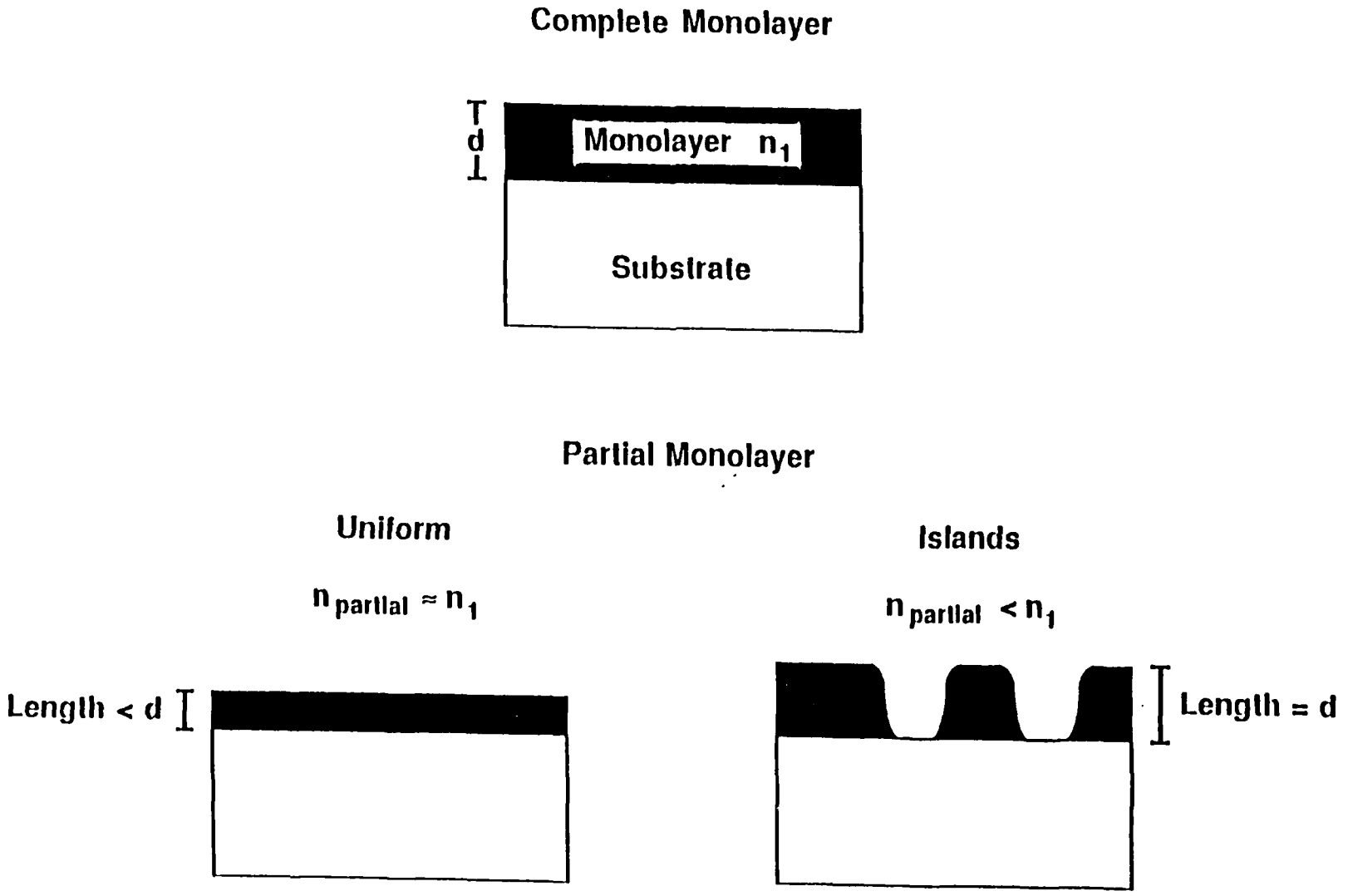
Complete Monolayer
d
Monolayer n_1
Substrate
Partial Monolayer
Uniform
$n_{partial} \approx n_1$
Length < d
Islands
$n_{partial} < n_1$
Length = d

between these possibilities, since we must assume the refractive index of the monolayer in order to determine its thickness. X-ray reflection can, however, differentiate between these two models. For a structure containing islands, the positions of the minima in the X-ray profile would be the same as those of the complete monolayer since the distances between the air-monolayer and monolayer-substrate interfaces would be the same. The intensities of these minima would change because the average electron density within the island-containing structure would be lower than that within the complete monolayer. For the "uniform" structure the distance separating the interfaces would be less than that of the complete monolayer. Therefore the locations of the minima would differ from those of the complete monolayer.

Figure 7 shows the intensity of X-rays reflected from two monolayers prepared from octadecyltrichlorosilane ($Cl_3Si(CH_2)_{17}CH_3$, OTS). The complete monolayer was prepared by immersing the silicon substrate in a solution containing OTS for 1 h. It had a thickness, by ellipsometry, of 26 Å. The second sample was placed in the same solution for 40 sec. By ellipsometry its thickness was 14 Å, approximately 60% of that of the complete structure. There is an obvious shift in the position of the primary minimum for the complete and partial monolayers. This shift corresponds to a difference of 7 Å in thickness, which is well beyond the experimental error of the experiment.

Figure 7. Comparison of the X-ray reflectivity, R/R_F, of partial and complete monolayers prepared from $Cl_3Si(CH_2)_nCH_3$. A) n = 17. B) n = 11. The reflectivities of the complete monolayers are offset by a factor of 100.

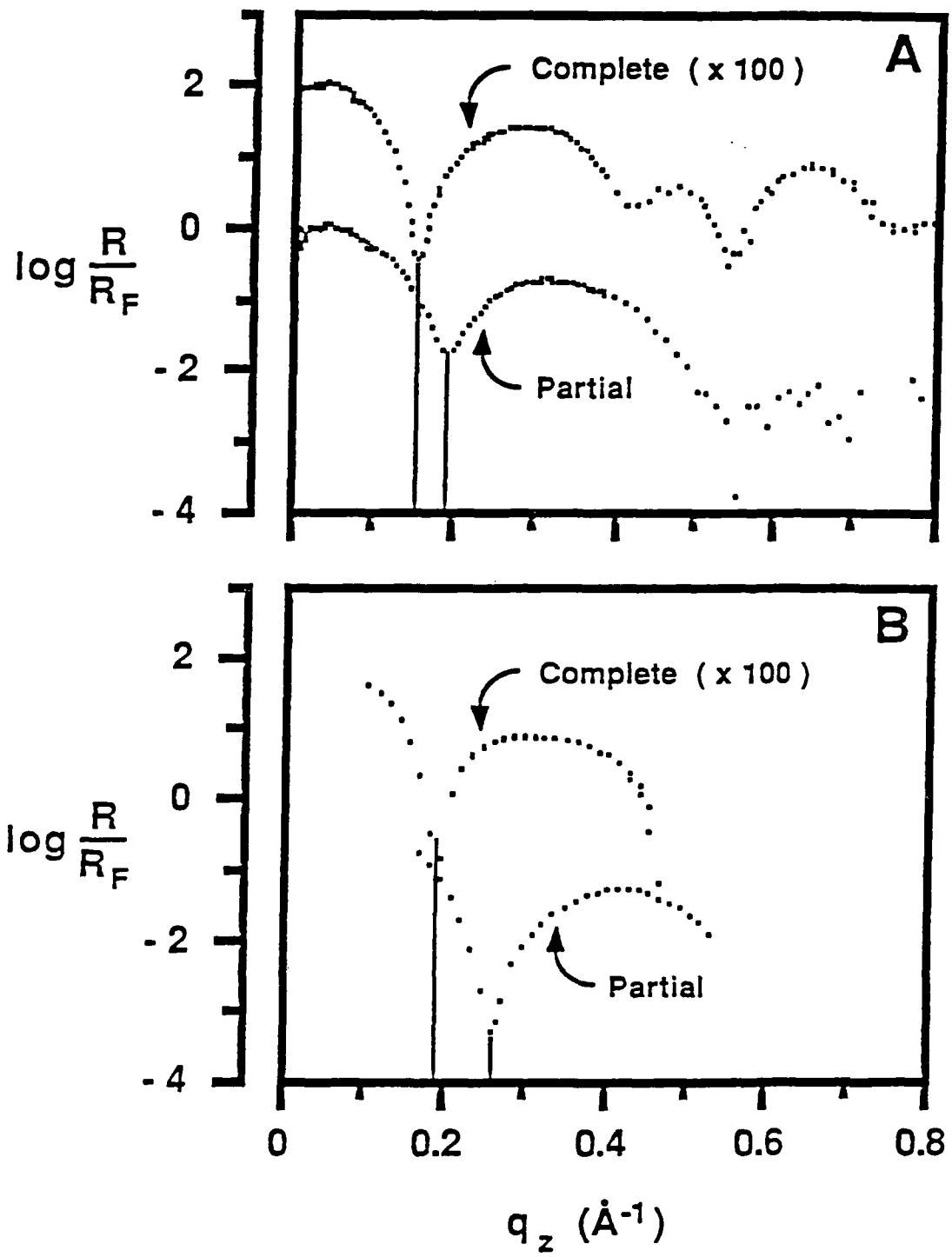
A
Complete (x 100)
Partial
B
Complete (x 100)
Partial
log R/R_F
2
0
-2
-4
0
0.2
0.4
0.6
0.8
q_z (Å^-1)

Figure 7 also presents similar data for two monolayers formed from dodecyltrichlorosilane ($Cl_3Si(CH_2)_{11}CH_3$). While this set of data is not as complete as that for the monolayers prepared from OTS, the shift in the location of the minimum for the partial monolayer is also readily apparent. While in this latter system the incompleteness of the data set prevented us from obtaining reliable values for the electron density of the monolayer, the similarity in the amplitudes of the minima suggests that the electron density of the incomplete monolayer was similar to that of the complete structure.

We conclude that the structure of these partial monolayers is best described by the "uniform" model (Figure 6).[76] This conclusion differs from that of Sagiv,[77] which is based on an infrared study of partial (~ 60%) and complete monolayers prepared from OTS on aluminum by procedures similar to those used here.

Variation of the Electron Density of the Monolayer. The intensity of reflected X-rays at the interference minima in the X-ray profile is smallest when the intensities of light reflected from the substrate-monolayer and monolayer-air interfaces are equal. This condition is met when the electron density of the monolayer is approximately halfway between that of the silicon substrate and air. If the electron density of the organic layer is too close to that of the substrate or of air, the incoming X-rays

see only one interface: that having a significant change in electron density.

We have demonstrated this effect by comparing the X-ray profiles for two monolayers formed from alkyltrichlorosilanes containing ten carbon atoms: $Cl_3Si(CH_2)_9CH_3$ and $Cl_3Si(CH_2)_2(CF_2)_7CF_3$ (Figure 8). The fluorinated silane should generate a monolayer whose electron density is close to that of the silicon substrate. The amplitude of the minimum is much lower for the fluorinated alkylsiloxane than for the hydrocarbon. (The positions of the minima are different since the fluorinated silane has two electron density regimes along the normal axis, one for the layer containing the two $-CH_2-$ groups and one for the layer containing the eight-carbon perfluorinated chain. The alkylsiloxane monolayer containing the $-(CH_2)_9CH_3$ group has a uniform electron density throughout the monolayer).

Monolayers composed of hydrocarbon have electron densities midway between that of silicon and air and are very amenable to investigation by X-ray reflection. For other systems, such as the fluorinated monolayer on silicon shown in Figure 8 or hydrocarbon monolayers on transition metal substrates or on water, the acquisition of useful results from X-ray reflectivity will generally require detailed analysis.

Characterization of Chemical Reactions Involving a Monolayer. We have begun to explore the use of X-ray reflectivity to study changes in the structures of monolayers

Figure 8. Effect of changing the electron density of the alkylsiloxane monolayer on the intensity of reflected X-rays, R/R_F. A) Si/SiO_2 substrate. B) Monolayer prepared from $Cl_3Si(CH_2)_2(CF_2)_7CF_3$. C) Monolayer prepared from $Cl_3Si(CH_2)_9CH_3$. A and B are offset by factors of 10^4 and 10^2 respectively.

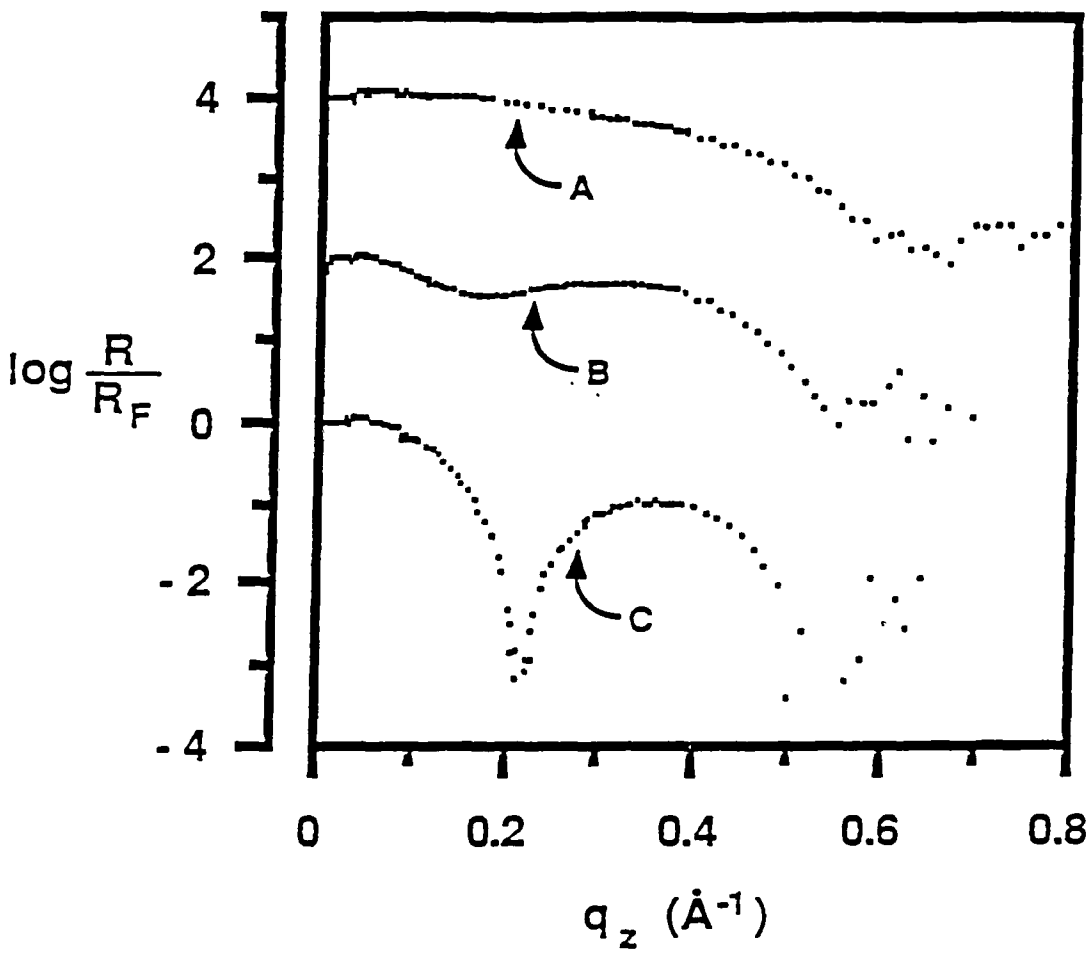
4
2
0
-2
-4
log R/R_F
A
B
C
0
0.2
0.4
0.6
0.8
q_z (Å^-1)

when chemical reactions alter their composition. We had two interests in these studies. First, we wished to determine if X-ray reflectivity had the sensitivity to provide a new analytical technique with which to follow reactions involving monolayers. We were especially interested in its ability to detect small changes in electron density (for example that accompanying oxidation of a $-CH=CH_2$ group to a $-CO_2H$ group). We were also concerned with its potential to damage the sample during analysis. Second, we wished to see if the structures of the alkylsiloxane monolayers were sufficiently rigid and well ordered that we could incorporate into them layers having large values of $\langle d\rho_{el}/dz \rangle$ (for example, by adding Br_2 to a $-CH=CH_2$ group to yield a $-CHBrCH_2Br$ moiety).

We have previously studied the addition of bromine to a monolayer prepared from $Cl_3Si(CH_2)_{15}CH=CH_2$ (HTS).[16] The contact angle of water on this vinyl-terminated monolayer was $\theta_a^{H_2O} = 100°$. Reaction with elemental bromine generated what we hypothesized to be the corresponding 1,2-dibromide (and other related brominated species)[78] and resulted in a decrease in $\theta_a^{H_2O}$ to ~ 80°. XPS spectra confirmed the incorporation of bromine into the monolayer. Ellipsometry suggested that the monolayer had lengthened by 2 - 3 Å.[79]

Figure 9 presents X-ray reflectivity data for the bromination of a monolayer prepared from HTS. Reflectivities were measured from a single monolayer before and after exposure to a solution of elemental bromine in CH_2Cl_2. After reaction, the primary minimum shifted to lower q_z

Figure 9. Change in the intensity of reflected X-rays that results from chemical transformations of vinyl-terminated alkylsiloxane monolayers prepared from $Cl_3Si(CH_2)_{15}CH=CH_2$ (HTS). A) Addition of elemental bromine (2%, v:v, in CH_2Cl_2) to form $-CHBrCH_2Br$ or related brominated structures. B) Oxidation by $KMnO_4$ (0.5 mM)/$NaIO_4$ (19.5 mM)/K_2CO_3 (1.8 mM, pH 7.5) to $-CO_2H$. For both A and B the upper X-ray profile, offset by a factor of 100, is that of the original monolayer; the lower is that after the transformation of the tail group of the monolayer.

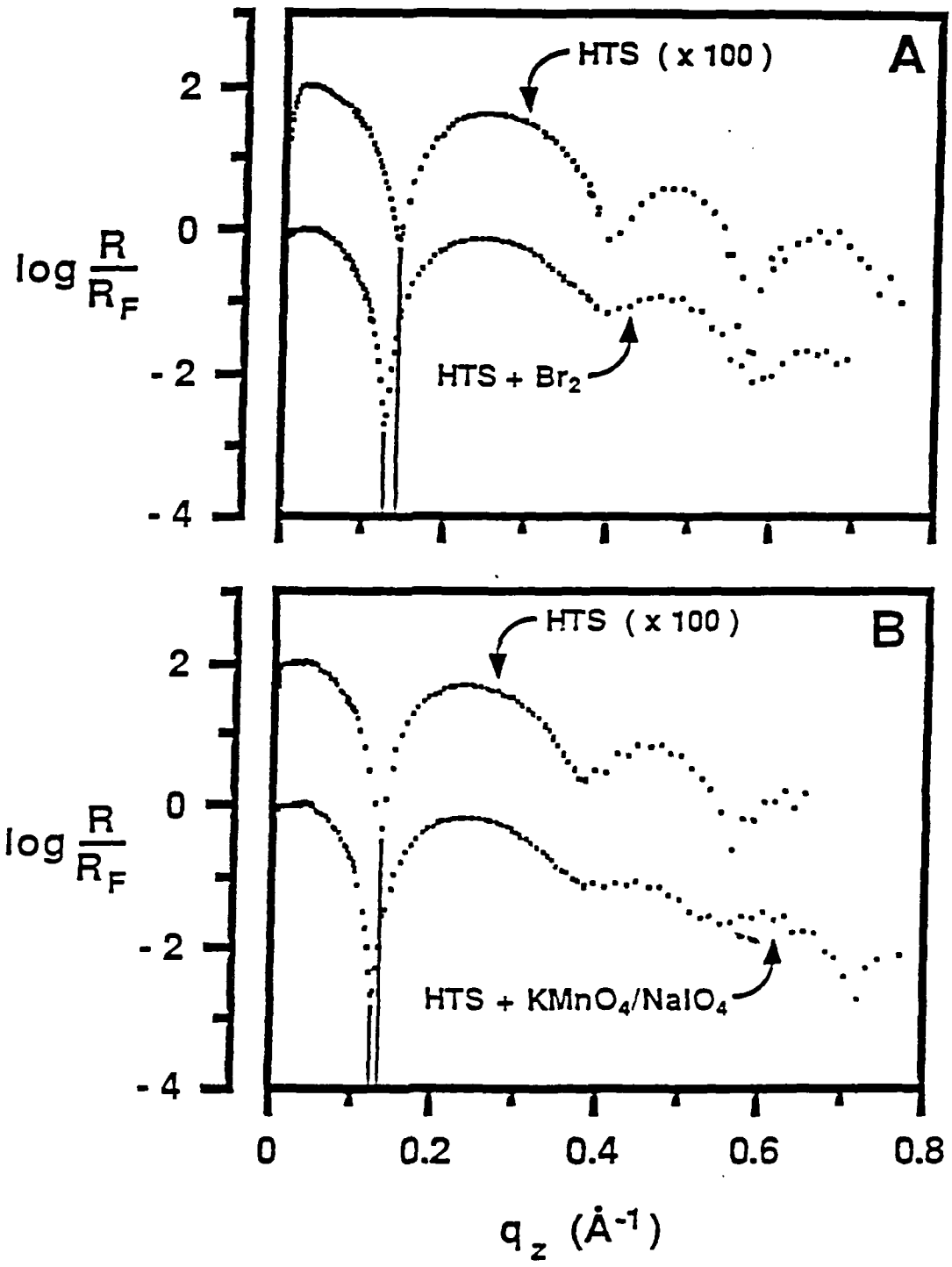
HTS (x 100)
A
2
0
- 2
- 4
log R/R_F
HTS + Br2
HTS (x 100)
B
2
0
- 2
- 4
log R/R_F
HTS + KMnO4/NaIO4
0
0.2
0.4
0.6
0.8
q_z (Å^-1)

(Δq_z = 0.014 $Å^{-1}$). Since the bromination effectively lengthens the monolayer by one atomic center,[80] this change is expected and is consistent with the ellipsometric data. The addition of one methylene unit to a saturated alkyl chain containing 17 carbon atoms would shift q_z by 0.0063 $Å^{-1}$.[81] The intensities of the minima also changed on bromination; the primary minimum deepened while the second decreased in amplitude.

If the bromine were localized in the position of the double bond in a trans-extended conformation for the organic chain, we would expect to infer from the X-ray reflectivity a layer approximately 4 Å thick with an electron density several times that of the hydrocarbon. Fitting the intensity data to a three-layer model did find a localized layer of high electron density. The best fit to the data, however, suggested a rather broad layer (6 Å (FWHM) in thickness) whose electron density corresponded to approximately 60% of that expected for complete bromination of the vinyl groups in the monolayer.

These results do not indicate a well-ordered, layered structure for the brominated monolayer derived from HTS.[82] Their interpretation is, however, complicated by X-ray damage to the brominated sample during the reflection measurements, by uncertainty concerning the structures formed on bromination, and by damage to the sample during the reflectivity measurements before reaction with bromine. After measuring the X-ray reflectivity of the vinyl-

terminated monolayer prior to bromination, the central region of the sample had a contact angle with water approximately 30° lower than the edges of the sample that were outside of the X-ray beam. After bromination, the central area of this sample had a contact angle of θ_a^{H2O} = 67°, 11° less than that of the edge (θ_a^{H2O} = 78°). Figure 10 presents XPS spectra for the brominated monolayer. The survey spectra indicate that there was only one-third as much bromine in the region exposed to the X-rays as in the section not exposed to the radiation. The C 1s spectra were also qualitatively different in these regions: the exposed area showed several different carbon environments with binding energies at least 3 eV higher than that of $-CH_2-$. Since the contact angles on the surface of the vinyl-terminated monolayer indicated some degree of radiation damage prior to the bromination of the monolayer, the reduced concentration of bromine that we observed probably reflects a combination of two effects: first, the radiation destroyed some fraction of the initial vinyl groups, and, second, the synchrotron radiation removed some of the bromine that had added to the remaining vinyl groups.[83,84]

Figure 9 presents analogous reflectivity data for materials obtained by oxidation with $KMnO_4$ and $NaIO_4$ of monolayers prepared from HTS. The expected product of this reaction is a carboxylic acid.[85] As for the bromination, we measured the reflectivity from a single monolayer before and after reaction. The X-ray data indicated a slight increase

Figure 10. XPS spectra of alkylsiloxane monolayers terminated with $-CHBrCH_2Br$ (and related brominated species, indicated by -"$CHBrCH_2Br$") and $-CO_2H$ groups after exposure to X-ray radiation from a synchrotron source: survey spectra (left) and high resolution spectra of the C 1s region (right). A) Edge of monolayer that was not exposed to any synchrotron X-ray radiation. B) Central area that was irradiated with the greatest flux of X-rays.

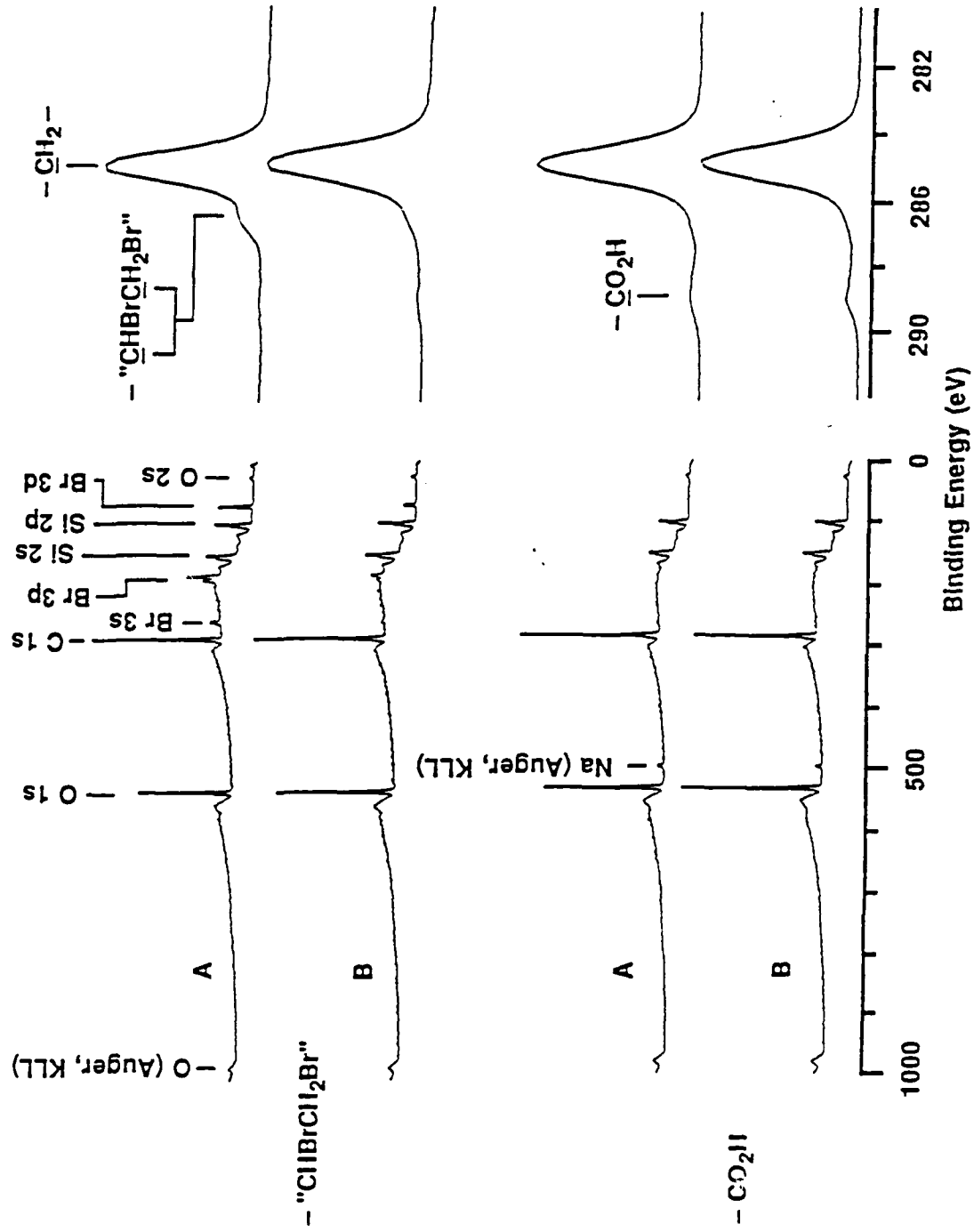
O (Auger, KLL)
O 1s
C 1s
Br 3s
Br 3p
Si 2s
Si 2p
O 2s
Br 3d
A
B
"ClIBrCl2Br"
Na (Auger, KLL)
A
B
CO2H
1000
500
0
Binding Energy (eV)
"CHBrCH2Br"
CH2
CO2H
290
286
282

in the thickness of the monolayer on oxidation, although this change in thickness was not as large ($\Delta q_z = 0.008$ Å^{-1}) as that observed on bromination. The second minimum was also reduced in amplitude after the oxidation. Since this reaction replaces a carbon atom with two oxygen atoms, but does not add to the end-to-end length of the chain, we do not expect the change in the thickness of the monolayer to be as large in this reaction as in the bromination reaction. Attempts to model the observed data suggested that there was a high density region at the air-monolayer interface. The agreement between the model and the data was, however, poor.

Contact angle measurements on the vinyl-terminated monolayer after the determination of its X-ray reflectivity revealed typical radiation damage. After the reflectivity measurements on the oxidized monolayer there was, however, no observable difference in the contact angles of water ($\theta_a^{H_2O} \approx 40°$) between the region of the sample which had been exposed to X-rays and the regions which had not. The XPS spectra (Figure 10) also show no difference between the irradiated and unirradiated regions. This apparent uniformity in the surface and the resulting implication that X-ray damage is not important in the these X-ray reflectivity experiments is reasonable but possibly misleading. Both the $KMnO_4/NaIO_4$ oxidation and the synchrotron radiation would be expected to generate oxidized species in the monolayer, and it might not be possible for us to detect radiation damage in this oxidized system.

Discussion

This work makes it possible to compare measurements of the thickness of alkylsiloxane monolayers on silicon using two techniques: optical ellipsometry and low-angle X-ray reflectivity. The former technique is more convenient than the latter, but its use requires certain assumptions whose correctness is difficult to check. The good agreement between results from these independent techniques strongly supports the accuracy of the thicknesses from ellipsometry. The small, systematic difference observed between these sets of results emphasizes the importance of detailed consideration of the structure and properties of the interfaces involved in reflecting light in the optical and X-ray regions of the spectrum.

Ultimately the correctness of ellipsometry relies on the proper choice for the refractive index of the monolayer. While the agreement between the X-ray and ellipsometric results is not sufficient to determine this index accurately, we note that the electron density of the monolayer is apparently independent of both the degree of completeness of the monolayer and the length of the alkyl group in the silane. Using the same refractive index for all samples, whether partial or fully formed, therefore appears justified. This conclusion differs from that reached for partial, "skeletized" films prepared by the etching of Langmuir-Blodgett multilayers, rather than the direct deposition of partially formed monolayers.[86,87] It is plausible that this

type of manipulation might yield an island structure rather than the apparently uniform partial monolayers studied here.

The information available from X-ray reflectivity concerning organic monolayer films is complementary to that available from other techniques. X-ray reflectivity requires no a priori assumptions about the structure (index of refraction, roughness, thickness) of the sample. It has a sensitivity to atomic scale structure that comes with the short wavelength of X-ray light. In addition, the ability of X-rays to penetrate solids makes it applicable to buried interfaces, even if the overlying film is not transparent in the optical spectrum.

X-ray reflectivity also has several limitations. First, it requires a suitably flat substrate. At present highly polished glass, float glass, and silicon are the only solids that have been shown to have satisfactory flatness,[88,89] although a number of liquids[49-51] and liquid crystals[52-54] have been examined with this technique. Recent progress in the epitaxial growth of metal surfaces[90] and the preparation of ultrasmooth surfaces[91] suggests that the extension of this technique to other substrates will soon be possible. Second, the electron density of the monolayer must be different from that of both the substrate and air; too close matching with either results in an ill-defined interface (that is, a small value of $\langle d\rho_{el}/dz \rangle$ at the interface) and a decrease in sensitivity and resolution. Third, organic samples may be damaged by exposure to high-intensity X-rays. Irradiation of

these monolayers in the presence of dioxygen appeared to result in oxidation. Exposure of monolayers containing C-Br bonds results in a loss of bromine. This type of loss is also observed during XPS analysis under conditions that do not damage methyl- or vinyl-terminated monolayers.[16] How important these damage processes are in causing artifacts in the data, and how effectively they can be suppressed by changing experimental conditions (for example, by using inert atmospheres or vacuum, low temperatures, or short exposure times) remains to be established. We believe that better control over the conditions under which X-ray reflectivity measurements are made will permit the use of this technique for the detailed analysis of the structure of monolayer systems.

Acknowledgments

This research was supported by the Office of Naval Research, the Defense Advanced Research Projects Agency (through the University Research Initiative), the National Science Foundation (Grant DMR 86-14003 to the Harvard Materials Research Laboratory), and the Joint Services Electronics Program of the Department of Defense (Grant N0014-84-K-0465). XPS spectra were obtained using instrumental facilities purchased under the DARPA/URI program and maintained by the Harvard University MRL. The Rotating Anode facility is part of the MRL. The synchrotron measurements were carried out at the National Synchrotron

Light Source (NSLS) at Brookhaven National Laboratory. Research at the NSLS is supported by the Office of Basic Energy Sciences, U. S. Department of Energy, under contract DE-AC02-76CH00016. Ian Tidswell was the recipient of a NATO studentship. We are grateful to Dr. David Osterman and Dr. Thomas Rabedeau for assistance in these experiments, to Dr. Abraham Ulman of Eastman Kodak for providing preprints of articles, and to Dr. Ralph Nuzzo of AT&T Bell Laboratories for helpful discussions.

Experimental Section

Materials. Decyl-, dodecyl-, tetradecyl-, hexadecyl-, and octadecyltrichlorosilane were obtained from Petrarch Systems and distilled prior to use. The compound 3,3,4,4,5,5,6,6,7,7,8,8,9,9,10,10,10-heptadecafluorodecyltrichlorosilane ($Cl_3Si(CH_2)_2(CF_2)_7CF_3$) was obtained from Petrarch and used as received. The synthesis of 16-heptadecenyltrichlorosilane (HTS) has been described previously.[16] Hexadecane and bicyclohexyl were obtained from Aldrich and purified by percolating twice through neutral, grade 1, activated (as purchased) alumina (Fisher). The purified solvents passed the Bigelow test for polar impurities.[92] Silicon (100) was obtained in 3 in. diameter wafers from Semiconductor Processing Corp (Boston, MA) (n-type, laser grade) in three thicknesses, 0.080 in., 0.125 in., and 0.200 in., and from Monsanto (p-type, 0.015 in). Water was passed through an ion exchanger (Cole-Parmer) and distilled in a Corning Model AG-1b glass distillation apparatus.

Preparation of Monolayers. The silicon wafers were cut into strips 1 in. wide. These strips were cleaned by heating in a solution of conc. H_2SO_4 and 30% H_2O_2 (70:30 v/v) at 90 °C for 30 min.[93] (CAUTION: 'piranha' solution reacts violently with many organic materials and should be handled with great care.) The substrates were rinsed thoroughly with distilled water and stored under water until use.

The cleaned silicon strips were removed from water using teflon-coated forceps (Pelco). All visible traces of water

were eliminated by exposing the sample to a stream of argon (minimum purity 99.995%) for ~ 30 sec. The silicon was then placed in a ~ 0.5% w:w solution of the alkyltrichlorosilane in hexadecane or bicyclohexyl. The containers for the solution were custom made from rectangular glass tubing that had one end sealed. Prior to use and during the formation of the alkylsiloxane monolayers, the containers were kept either under a dry nitrogen atmosphere or in a desiccator containing P_2O_5 (Baker, "granusic"). After 1 h (desiccator) or 24 h (nitrogen atmosphere), the substrate was removed from solution and placed in 100 mL of $CHCl_3$ for 15 min to remove any microscopic contaminants that might have adsorbed onto the surface of the monolayer. The sample was then immersed in 100 mL of ethanol for 30 sec and rinsed with ethanol dispensed from a 2-mL disposable pipette. The monolayer was dried under a stream of argon and measurements of contact angle and ellipsometry were made immediately.

Contact Angles. Advancing contact angles were determined on sessile drops using a Ramé-Hart Model 100 contact angle goniometer equipped with a controlled environment chamber. The relative humidity in the chamber was maintained at > 80% by filling the wells of the sample chamber with water. The temperature was not controlled and varied from 20 to 25 °C. The volume of the drop used was 3 μL; its pH was ~ 5.6. All reported values are the average of at least four measurements on the film surface and have a maximum range of ± 3°.

Ellipsometry. Ellipsometric measurements were made with a Rudolph Research Model 43603-200E thin film ellipsometer. The light source was a He-Ne laser (λ = 6328 Å). The angle of incidence was 70.0° (relative to the normal of the plane of the sample) and the compensator was set at -45.0°. The measurements necessary for the calculation of the film thickness consisted of the determination of the polarizer and analyzer angles for the silicon substrate and the corresponding set of angles for the substrate coated with a monolayer film.

Each set of analyzer and polarizer readings, measured in zones 1 and 3,[94] were the average of at least four measurements taken at different locations (separated by at least 1 cm) on the sample. The angles that comprised this average had a maximum scatter of $\pm$ 0.15°. These measurements were determined in air for the bare substrate within 5 min of its removal from water. The substrate was placed in the solution of alkyltrichlorosilane immediately after these measurements. Measurements for the substrate-monolayer systems were taken no more than 5 min after the samples had been washed with ethanol.

The refractive index of the substrate was calculated from the analyzer and polarizer angles for the uncoated silicon. This value was then used to determine the thickness of the monolayer according to the algorithm of McCrackin.[29] The lengths were calculated assuming that the monolayer had a refractive index of 1.45. The algorithm calculated two

values for the length of the monolayer, both of which were complex. Since the length of the monolayer must be real, we chose the real part of the complex number with the smaller imaginary component as the thickness of the monolayer. (The other choice was inherently unreasonable since it was greater than 1000 Å.) Thicknesses determined in this way are accurate to ± 2 Å.

X-Ray Photoelectron Spectroscopy. The XPS spectra were obtained using a Surface Science Laboratories Model SSX-100 spectrometer (monochromatized Al $K\alpha$ X-ray source; 10^{-8}-10^{-9} torr) referenced to Au $4f_{7/2}$ at 84.0 eV. Samples were washed with ethanol, dried under a stream of argon, and introduced into the spectrometer. For each sample a survey spectrum (resolution 1.1 eV, spot size 1000 μm, 1 scan) and high resolution spectra of the peaks for C 1s, O 1s, Br 3d, and Si 2p (resolution 0.16 eV, spot size 300 μm, 10-30 scans) were collected. Atomic compositions were determined using standard multiplex fitting routines with the following sensitivity factors: C 1s, 1.00; O 1s, 2.49; Si 2p, 0.90; Br 3d, 3.188.[95]

X-Ray Reflection Measurements. X-ray sources were a Rigaku rotating anode (RA) X-ray generator (Cu $K\alpha_1$ radiation, λ = 1.54 Å, 90 mA, 45 keV) and the National Synchrotron Light Source (NSLS) at Brookhaven National Laboratory (beam line X-22B, λ = 1.71 Å). Monochromatic radiation was obtained by reflection from a monochromator (RA, triple bounce Germanium (111); NSLS, single bounce Germanium (111)). The beam size

was 0.1 x 5 mm for incident angles less than 1° and 0.5 x 5 mm for incident angles greater than 1°. X-rays were monitored using two scintillation detectors: one for the incoming beam, the other for the radiation reflected from the sample. The intensities of the reflected X-rays were normalized to the intensity of the incoming beam.

Since the background radiation was a function of the angle of the incoming beam, point by point background subtraction was performed. The background was determined by purposely misaligning the detector by $\pm$ 0.3° at each incident angle θ.

Samples were mounted in a brass cell with Kapton™ (DuPont) windows. The chamber excluded X-rays at angles greater than 7°. The atmosphere in the chamber was either air or helium.

The range of intensities that could be detected was 10^6 with the rotating anode and 10^9 at NSLS. A typical reflection scan required 15 h on the rotating anode and 4 h at NSLS. The data that was obtained at NSLS covered twice the range in q_z as that from the rotating anode.

Bromination. The X-ray reflectivity for a monolayer prepared from HTS was measured as above. This monolayer was then placed in a 2% (by volume) solution of elemental bromine in CH_2Cl_2 for 7 h. The wafer was then rinsed in CH_2Cl_2 and in ethanol. The reflectivity was then measured again.

Oxidation. As for the bromination, the reflectivities before and after oxidation were measured as described above.

Stock solutions of $KMnO_4$ (5 mM), $NaIO_4$ (195 mM), and K_2CO_3 (18 mM) in water were prepared. Immediately prior to the oxidation 1 mL of each of these solutions was combined with 7 mL of distilled water to create the oxidizing solution ($KMnO_4$, 0.5 mM; $NaIO_4$, 19.5 mM; K_2CO_3, 1.8 mM, pH 7.5). The monolayer prepared from HTS was placed in this solution for 2 h at 75 °C. The sample was removed from the oxidant and rinsed in 20 mL of each of $NaHSO_3$ (0.3 M), water, 0.1 N HCl, water, and ethanol.

Pentadecyltrichlorosilane. Dihydrogenhexachloroplatinate(II) (Alfa, 5.3 mL of a 0.01 M solution in THF, 0.053 mmol), trichlorosilane (Petrarch, 8.6 mL, 85 mmol) and 1-pentadecene (Aldrich, 15.01 g, 71 mmol) were placed under argon in a dry heavy-walled glass tube (diameter-2.5 cm, length-21 cm) equipped with a sidearm and a 0-10 mm PTFE stopcock. The solution was degassed (freeze-pump-thaw, 3 cycles) and the tube was sealed under vacuum at -195 °C. The tube was then warmed to room temperature, after which it was heated in an oil bath (99 °C, 43 h). The tube was then cooled to room temperature. The reaction solution was transferred to a 100-mL round-bottomed flask equipped with a vacuum adapter. A liquid nitrogen-cooled trap was attached and the excess trichlorosilane and THF were removed by a trap-to-trap distillation. The remaining liquid was distilled in a dry Kugelrohr distillation apparatus. The product (15.3 g, 44 mmol, 62%) was the fraction collected from 95 °C(0.013 torr) to 105 °C(0.010 torr).

^{1}H NMR ($CDCl_3$): δ 1.7-1.2 (m, 28), 0.9 (t, 3). ^{13}C NMR ($CDCl_3$): δ 32.24, 32.01, 30.00, 29.94, 29.89, 29.68, 29.25, 24.50, 22.98, 22.51, 14.29. Anal. Calcd. for $C_{15}H_{31}Cl_3Si$: C, 52.08; H, 9.05; Cl, 30.75. Found: C, 51.89; H, 9.12; Cl, 30.95.

References and Notes

1. Azzam, R. M. A.; Bashara, N. M. Ellipsometry and Polarized Light; North-Holland Publishing Company: Amsterdam, 1977 and the references cited therein.

2. Gun, J.; Iscovici, R.; Sagiv, J. J. Colloid Interface Sci. **1984**, 101, 201-213.

3. Porter, M. D.; Bright, T. B.; Allara, D. L.; Chidsey, C. E. D., J. Am. Chem. Soc. **1987**, 109, 3559-3568.

4. Troughton, E. B.; Bain, C. D.; Whitesides, G. M.; Nuzzo, R. G.; Allara, D. L.; Porter, M. D. Langmuir **1988**, 4, 365-385.

5. Allara, D. L.; Nuzzo, R. G. Langmuir **1985**, 1, 45-52.

6. Pershan, P. S. Proc. Natl. Acad. Sci. U. S. A. **1987**, 84, 4692-4693.

7. Pomerantz, M.; Segmüller, A. Thin Solid Films **1980**, 68, 33-45.

8. Pomerantz, M.; Segmüller, A.; Netzer, L.; Sagiv, J. Thin Solid Films **1985**, 132, 153-162.

9. Richardson, R. M.; Roser, S. J. Liq. Crys. **1987**, 2, 797-814.

10. Wolf, S. G.; Leiserowitz, L.; Lahav, M.; Deutsch, M.; Kjaer, K.; Als-Nielsen, J. Nature **1987**, 328, 63-66.

11. Helm, C. A.; Möhwald, H.; Kjaer, K.; Als-Nielsen, J. Europhys. Lett. **1987**, 4, 697-703.

12. Parratt, L. G. Phys. Rev. **1954**, 95, 359-369.

13. Bartell, L. S.; Betts, J. E. J. Phys. Chem. **1960**, 64, 1075-1076.

14. Miller, J. R.; Berger, J. E. J. Phys. Chem. **1966**, 70, 3070-3075.

15. Smith, T. J. Opt. Soc. Am. **1968**, 58, 1069-1079.

16. Wasserman, S. R.; Tao, Y-T.; Whitesides, G. M. Langmuir, in press.

17. Bain, C. D.; Whitesides, G. M. J. Phys. Chem. in press.

18. Maoz, R.; Sagiv, J. J. Colloid Interface Sci. **1984**, 100, 465-496.

19. Abel, E. W.; Pollard, F. H.; Uden, P. C.; Nickless, G.; J. Chromatog. **1966**, 22, 23-28.

20. van Roosmalen, A. J.; Mol, J. C. J. Phys. Chem. **1979**, 83, 2485-2488.

21. Kallury, K. M. R.; Krull, U. J.; Thompson, M. Anal. Chem. **1988**, 60, 169-172.

22. Zhuravlev, L. T. Langmuir **1987**, 3, 316-318.

23. Madeley, J. D.; Richmond, R. C. Z. anorg. allg. Chem. **1972**, 389, 92-96.

24. Water seems to be necessary for the formation of alkylsiloxane monolayers. When prepared in a dry nitrogen atmosphere, the preparation of a complete monolayer requires longer times of immersion (~ 5 h) than when the process is performed in the ambient laboratory environment (~ 30 min).

25. Born, M.; Wolf, E. Principles of Optics, 6th ed.; Pergamon Press: Oxford, 1980; Chapter 1.

26. Tillman, N.; Ulman, A.; Schildkraut, J. S.; Penner, T. L. J. Am. Chem. Soc. **1988**, 110, 6136-6144.

27. Tidswell, I. M.; Ocko, B. M.; Pershan, P. S.; Axe, J. D.; Wasserman, S. R.; Whitesides, G. M. Phys. Rev. B, submitted.

28. The inherent curvature of these thin substrates made it necessary, for the X-ray reflectivity measurements, to continually monitor the direction of the axis normal to the plane of the monolayer.

29. McCrackin, F. L.; Passaglia, E.; Stromberg, R. R.; Steinberg, H. L. J. Res. Natl. Bur. Stand., Sect A. **1963**, 67, 363-377.

30. The refractive index of the Si/SiO_2 substrate varied slightly from sample to sample. The observed range of refractive indices was 3.84-3.89. The thicknesses of monolayers reported here were determined using the refractive index of the substrate on which that monolayer was prepared.

31. The contact angles of water and hexadecane on the bare substrate were $\theta_a^{H_2O} \approx 0°$; $\theta_a^{HD} \approx 0°$. The contact angles for monolayers prepared from octadecyltrichlorosilane (OTS) were $\theta_a^{H_2O} = 112°$; $\theta_a^{HD} = 42°$.

32. Infrared spectroscopy using polarized radiation suggests that these monolayers are oriented nearly perpendicular to the surface (tilt angle $\approx 14 \pm 18°$). See references 18 and 26.

33. Our experimental protocol (see experimental section) measured the ellipsometric constants of the substrate within 5 min of removal of the silicon wafer from the water in which it had been stored. Using the X-ray reflection technique we have observed the slow (20-25 Å in 24 h) buildup of a contaminating layer on a bare Si/SiO_2 substrate.

34. Carim, A. H.; Dovek, M. M.; Quate, C. F.; Sinclair, R.; Vorst, C. Science **1987**, 237, 630-632.

35. Carim, A. H.; Sinclair, R. Mater. Lett. **1987**, 5, 94-98.

36. A demonstration of the validity of the use of an effective index of refraction for the substrate is found in reference 1, pp 332-340.

37. Fenstermaker, C. A.; McCrackin, F. L. Surface Sci. **1969**, 15, 85-96.

38. Smith, T. Surface Sci. **1976**, 56, 252-271.

39. The substrates used in this study had a surface roughness on the order of 3-4 Å. See reference 27.

40. The simultaneous determination of the refractive index and length of the monolayer depends on the precision of the

ellipsometric measurement. For the films studied here all refractive indices between 1.0 and 2.5 are possible for the index of the monolayer. See reference 29.

41. A transparent medium does not absorb light and has a real refractive index.

42. CRC Handbook of Chemistry and Physics, 56th ed.; Weast, R. C., Ed.; CRC Press: Cleveland, Ohio, 1975.

43. Polymer Handbook; Brandrup, J. and Immergut, E. H., Ed.; John Wiley: New York, 1975; v-13 - v-22.

44. Nyburg, S. C.; Lüth, H. Acta Cryst. **1972**, B28, 2992-2995.

45. Crissman, J. M.; Passaglia, E.; Eby, R. K.; Colson, J. P. J. Appl. Cryst. **1970**, 3, 194-195.

46. The average electron density in these monolayers was ~ 0.30 $Å^{-3}$. This value is slightly less than that of crystalline n-paraffins (0.32 $Å^{-3}$). The latter value was calculated from the crystal structures of octadecane ($C_{18}H_{38}$) and eicosane ($C_{20}H_{42}$) given in references 44 and 45.

47. We can obtain an approximate value for the refractive index of the monolayer using the electron density of the monolayer, ρ_{el}, determined by the X-ray reflectivity

measurements. This electron density can be converted to a mass density, ρ_m. An alternate form of equation 7 (see discussion on the projected area of alkylsiloxane groups) is given by equation i where V is the volume of each hydrocarbon

$$V = Ad = \frac{N_e}{\rho_{el}} \qquad \text{(i)}$$

$$\frac{n^2 - 1}{n^2 + 2} = \frac{R\rho_m}{W} \qquad \text{(ii)}$$

tail in the monolayer. Since the mass of each tail, m, is simply the sum of the masses of each atom in the tail, the mass density of the monolayer can be calculated. The refractive index of a substance is related to its molar refractivity, R, mass density, and molecular weight, W, by equation ii. R is found by summing the refractivities of each methylene and methyl group in the hydrocarbon tails (Vogel, A. I. J. Chem. Soc. **1948**, 1833-1855). This calculation yields an approximate refractive index of 1.50 ± 0.07.

48. The change in thickness of the monolayer as a function of its assumed refractive index is a linear function of the length of the monolayer: the longer the monolayer, the greater the change in the calculated thickness.

49. Braslau, A.; Deutsch, M.; Pershan, P. S.; Weiss, A. H.; Als-Nielsen, J.; Bohr, J. Phys. Rev. Lett. **1985**, 54, 114-117.

50. Bosio, L.; Oumezine, M. J. Chem. Phys. **1984**, 80, 959-960.

51. Sluis, D.; Rice, S. A. J. Chem. Phys. **1983**, 79, 5658-5672.

52. Ocko, B. M.; Braslau, A.; Pershan, P. S.; Als-Nielsen, J.; Deutsch, M. Phys. Rev. Lett. **1986**, 57, 94-97.

53. Ocko, B. M.; Pershan, P. S.; Safinya, C. R.; Chiang, L. Y. Phys. Rev. A **1987**, 35, 1868-1872.

54. Pershan, P. S.; Braslau, A.; Weiss, A. H.; Als-Nielsen, J. Phys. Rev. A **1987**, 35, 4800-4813.

55. Als-Nielsen, J. Physica **1986**, 140A, 376-387.

56. ρ_{el} is the volume density of electrons: that is, the number of electrons present in a unit volume.

57. The momentum, p, of a photon is $p = h/\lambda$. Since h is a constant, momentum can be represented by λ^{-1}, which has units of $Å^{-1}$.

58. The index of refraction toward X-rays, n, is given by equation iii. This relation is derived from the classical

$$n = 1 - (2\pi)^{-1}\lambda^2\rho_{el}r_o \qquad r_o = 2.818 \times 10^{-5}\ \text{Å} \qquad \text{(iii)}$$

theory of dispersion for frequencies much higher than the resonance frequencies of the electrons in the sample. See reference 25, Chapter 2.

59. See appendix in supplementary material.

60. Halliday, D.; Resnick, R. Physics, 3rd ed., Part 2; John Wiley: New York, 1978; Section 45-5.

61. Descriptions of this model and more sophisticated models for the structure of alkylsiloxane monolayers are found in reference 27.

62. From the mass densities of silicon and quartz we calculate electron densities of 0.70 $Å^{-3}$ and 0.80 $Å^{-3}$ respectively. Several mineral forms of silica, including opal and cristobalite, have densities 15% less than that of quartz. See reference 42.

63. Inclusion of a third layer for the silicon dioxide on the substrate improves the overall agreement between the observed reflectivity and that predicted by the model, but does not have a significant effect on the measured thickness of the monolayer. The presence of this layer in the model alters

the calculated thickness by no more than 0.5 Å. See reference 27.

64. We refer to σ_1 and σ_2 as the roughnesses of the two interfaces in our model. They actually provide a measure of the distances over which the refractive index changes from n_0 (or n_1) to n_1 (or n_2).

65. Two samples were analyzed under a helium atmosphere. Similar damage was observed for these samples as for those analyzed under air. The chamber holding the sample was not, however, air tight.

66. The binding energies, relative to $-CH_2-$, for oxidized carbon atoms are: $-\underline{C}H_2OH$, +1.5 eV; $-\underline{C}O-$, +3.0 eV; $-\underline{C}O_2H$, +4.5 eV. Gelius, U.; Hedén, P. F.; Hedmon, J.; Lindberg, B. J.; Manne, R.; Nordberg, R.; Nordling, C.; Siegbahn, K. Physica Scripta **1970**, 2, 70-80.

67. We were able to cause damage to these monolayers with a rotating anode by placing a monolayer in the direct beam of the anode for 24 h. The flux of this beam was ~ 1/10th that of the monochromatized radiation from the synchrotron. While the contact angle in the irradiated region decreased ($\theta_a^{H_2O} \approx 80°$), XPS failed to find a significant surface concentration of oxidized carbon atoms.

68. Sample deterioration will be important, however, in more detailed studies of how monolayer structure changes under various conditions.

69. Taft, E. A. J. Electrochem. Soc. **1978**, 125, 968-971.

70. The size of the silicon atom is taken as half the sum of the projections of the Si-O (1.33 Å) and Si-C (1.52 Å) bonds onto the z axis. These projections were calculated from standard bond lengths assuming a bond angle of 109.5°.

71. This value for the critical angle is slightly higher than the value $\theta_c = 0.221$ predicted by the electron density of crystalline silicon (0.70 A^{-3}). We attribute this discrepancy to curvature in the sample. See reference 27.

72. The electron density of the monolayer, 0.30 ± 0.03 $Å^{-3}$, calculated using the theoretical critical angle for silicon (ref. 69), corresponds to a mass density of 0.87 ± 0.10 g/cm^3. This density is calculated assuming that the monolayer consists solely of methylene groups.

73. The number of electrons in each constituent molecule of the monolayer was found by adding the number of electrons contributed by each atom in the tail of the silane, six for each carbon atom and one for each hydrogen.

74. The major source of uncertainty in this estimate is the uncertainty in the electron density of the monolayer.

75. Gaines, G. L., Jr. Insoluble Monolayers at Liquid-Gas Interfaces; Interscience: New York, 1966 and references cited therein.

76. We do not generalize this result to other monolayer systems. The alkyltrichlorosilanes form a monolayer through the creation of covalent silicon-oxygen bonds between the silane and the substrate. Once bound to the substrate the molecules cannot move along the surface. For systems such as thiols on gold, where the monolayer is held on the substrate by weaker interactions, it may be possible for the monolayer constituents to diffuse laterally across the surface.

77. Cohen, R. R.; Naaman, R.; Sagiv, J. J. Phys. Chem. **1986**, 90, 3054-3056.

78. Because of the high density of vinyl groups at the air-monolayer interface, bromination of these groups could conceivably induce some polymerization of the type presented in equation iv.

$$-CH{=}CH_2 + CH_2{=}CH- \xrightarrow{Br_2} -CHBr-CH_2-CH_2-CHBr- \qquad \text{(iv)}$$

79. In using ellipsometry to follow reactions we continued to use a refractive index of 1.45. This approach is clearly arbitrary, but we have found that even using the refractive index of elemental bromine (1.66) to describe the new layer on the surface alters our estimate of the change in thickness by only ~ 0.4 Å.

80. The van der Waals radius of bromine (1.95 Å) is slightly less than the sum of the covalent radii of carbon (0.77 Å) and hydrogen (0.371 Å) and the van der Waals radius of hydrogen (1.2 Å). The volume occupied by a bromine atom is therefore similar to that of a methyl group. Lange's Handbook of Chemistry, 11th ed.; Dean, J. A., Ed.; McGraw-Hill: New York, 1973.

81. We have calculated the expected change in q_z using the assumption that the monolayer-air and monolayer-substrate interfaces are perfectly sharp. In the appendix (see supplementary material) we show that this assumption yields the usual condition for destructive interference (eq J). For the primary minimum in R, n in equations H, I, and J is zero. Rearrangement of equation H with n = 0 results in equation v

$$q_{z_O} = \pi/d \qquad (v)$$

for the location of the primary minimum, q_{z_O}, as a function of d, the distance between the two interfaces. Values for d

were calculated using standard bond lengths and a bond angle of 109.5°.

82. While angle-resolved XPS studies might shed some light on the distribution of bromine within the monolayer, we have had difficulty obtaining reproducible results from brominated monolayers which were not exposed to synchrotron radiation. See reference 16.

83. We have observed a decrease in the intensity of the bromine signal during the accumulation of the XPS spectra. While the flux of X-rays in the spectrometer is unknown, it is certainly less than that of the X-ray beam from the synchrotron.

84. The binding energy of the bromine in the damaged region (Br $3d_{5/2}$, 70.5 eV) was identical to that in the areas unexposed to the X-rays.

85. Lemieux, R. U.; von Rudloff, E. Can. J. Chem. **1955**, 33, 1701-1709.

86. Blodgett, K .B.; Langmuir, I. Phys. Rev. 1937, 51, 964-982.

87. Tomar, M. S. J. Phys. Chem. 1974, 78, 947-950.

88. Cowley, R. A.; Ryan, T. W. J. Phys. D **1987**, 20, 61-68.

89. Materials such as cleaved mica or graphite may have suitable flatness for the application of the X-ray reflection technique, but they have not yet been developed for this purpose.

90. Hallmark, V. M.; Chiang, S.; Rabolt, J. F.; Swalen, J. D.; Wilson, R. J. Phys. Rev. Lett. **1987**, 59, 2879-2882.

91. Brown, N. J., Ann. Rev. Mater. Sci. **1986**, 16, 371-388.

92. Bigelow, W. C.; Pickett, D. L.; Zisman, W. A. J. Colloid. Sci. **1946**, 1, 513-538.

93. Pintchovski, F.; Price, J. B.; Tobin, P. J.; Peavey, J.; Kobold, K. J. Electrochem. Soc. **1979**, 126, 1428-1430.

94. See reference 29 for the definitions of the angular zones used in ellipsometry.

95. These XPS sensitivities are those supplied by Surface Science Laboratories in their ESCA 8.0B software. These values are those calculated by Scofield, corrected for the dependence of the mean free path of an electron on its energy. Scofield, J. H. J. Electron Spectrosc. **1976**, 8, 129-137.

Captions

Figure 1. Two-layer model used for ellipsometry. The silicon substrate has refractive index n_2, the monolayer has refractive index n_1, and the ambient air has refractive index n_0. The interfaces between each layer are assumed to be perfectly sharp. For the alkylsiloxane monolayers on silicon n_2 is ~ 3.8, n_1 is ~ 1.45, and n_0 is assumed to be 1. The incident angle of the laser light, ϕ_0, is 70°. The angles of refraction, $\phi_1 \approx 40°$ and $\phi_2 \approx 15°$, are given by Snell's law ($n_1 \sin\phi_1 = n_2 \sin\phi_2$).

Figure 2. Intensity, R, of X-rays reflected from alkylsiloxane monolayers on silicon-silicon dioxide substrates as a function of q_z, the momentum change of the photon upon reflection. The monolayers were prepared from alkyltrichlorosilanes, $Cl_3Si(CH_2)_nCH_3$. The top spectrum is for bare Si/SiO_2. Each spectrum is offset by 10^3 from the one above it. The solid line is the calculated Fresnel reflectivity, R_F, for a perfectly smooth silicon substrate.

Figure 3. Models for ρ_{el}, the electron density, and $d\rho_{el}/dz$, the change in electron density along the normal perpendicular to the plane of the monolayer, used to analyze the measured X-ray reflectivity of alkylsiloxane monolayers on Si/SiO_2 substrates. The air-monolayer and monolayer-substrate interfaces are represented in $d\rho_{el}/dz$ by Gaussian functions, $A_1\exp(z^2/2\sigma_1^2)$ and $A_2\exp((z-d)^2/2\sigma_2^2)$. The parameter d, the separation between the centers of these functions, represents the distance between the air-monolayer and monolayer-substrate interfaces. This distance is the thickness of the monolayer. A_1, A_2, σ_1, and σ_2 are the heights and widths of the Gaussian functions. The parameters $\delta\rho_1$ and $\delta\rho_2$ are the changes in refractive index across each interface and are proportional to $A_1\sigma_1$ and $A_2\sigma_2$. The electron density decreases from substrate to monolayer to air. The index of refraction for X-rays is a linear function of the electron density.

Figure 4. XPS spectra of a monolayer prepared from $Cl_3Si(CH_2)_{11}CH_3$ showing radiation damage caused by exposure to X-rays from a synchrotron source: survey spectra (left) and high resolution spectra of the C 1s region (right). A) Edge of sample unexposed to X-rays. The contact angle in this region was $\theta_a^{H_2O} = 112°$. The contact angle and XPS spectra of this area were indistinguishable from those of monolayers that had not been exposed to any X-ray radiation. No carbon atoms in oxidized environments are observed. B) Central area of sample exposed to the greatest flux of X-rays. The contact angle in this region was $\theta_a^{H_2O} = 82°$. The high-resolution C 1s spectrum exhibits a tail to higher binding energy, indicating the presence of oxidized carbon species.

Figure 5. Comparison of the thicknesses of alkylsiloxane monolayers as measured by ellipsometry and X-ray reflectivity. The solid circles (●) are the thicknesses of complete monolayers; the open circles (○) are the thicknesses of partial monolayers. The solid line is that expected if the two techniques yield the same thickness. The dotted line is offset by 1.4 Å and is that expected if only ellipsometry includes the

silicon atom of the alkylsilane in the measured thickness (see text).

Figure 6. Models for the structure of incomplete monolayers. A complete monolayer has a thickness, d, and an index of refraction, n_1. In the uniform model the partial monolayer has a length less than d and an index of refraction approximately equal to n_1. In the island model the incomplete monolayer has a thickness, d, but the index of refraction is less than n_1.

Figure 7. Comparison of the X-ray reflectivity, R/R_F, of partial and complete monolayers prepared from $Cl_3Si(CH_2)_nCH_3$. A) n = 17. B) n = 11. The reflectivities of the complete monolayers are offset by a factor of 100.

Figure 8. Effect of changing the electron density of the alkylsiloxane monolayer on the intensity of reflected X-rays, R/R_F. A) Si/SiO_2 substrate. B) Monolayer prepared from $Cl_3Si(CH_2)_2(CF_2)_7CF_3$. C) Monolayer prepared from $Cl_3Si(CH_2)_9CH_3$. A and B are offset by factors of 10^4 and 10^2 respectively.

Figure 9. Change in the intensity of reflected X-rays that results from chemical transformations of vinyl-terminated alkylsiloxane monolayers prepared from $Cl_3Si(CH_2)_{15}CH{=}CH_2$ (HTS). A) Addition of elemental bromine (2%, v:v, in CH_2Cl_2) to form $-CHBrCH_2Br$ or related brominated structures. B) Oxidation by $KMnO_4$ (0.5 mM)/$NaIO_4$ (19.5 mM)/K_2CO_3 (1.8 mM, pH 7.5) to $-CO_2H$. For both A and B the upper X-ray profile, offset by a factor of 100, is that of the original monolayer; the lower is that after the transformation of the tail group of the monolayer.

Figure 10. XPS spectra of alkylsiloxane monolayers terminated with $-CHBrCH_2Br$ (and related brominated species, indicated by -"$CHBrCH_2Br$") and $-CO_2H$ groups after exposure to X-ray radiation from a synchrotron source: survey spectra (left) and high resolution spectra of the C 1s region (right). A) Edge of monolayer that was not exposed to any synchrotron X-ray radiation. B) Central area that was irradiated with the greatest flux of X-rays.

The Structure of Self-Assembled Monolayers of Alkylsiloxanes on Silicon: A Comparison of Results from Ellipsometry and Low-Angle X-Ray Reflectivity

Stephen R. Wasserman and George M. Whitesides*
Department of Chemistry, Harvard University, Cambridge, MA 02138

Ian M. Tidswell, Ben M. Ocko, and Peter S. Pershan*
Division of Applied Sciences and Department of Physics, Harvard Univeristy, Cambridge, MA 02138

John D. Axe
Department of Physics, Brookhaven National Laboratory, Upton, NY 11973

Supplementary material: Appendix

Appendix

The general description of the intensity of X-rays reflected from a sample is given in equations A and B.[1] We will consider the form of the X-ray reflectivity, R, for two

$$R = R_F \left| \rho_\infty^{-1} \int_{-\infty}^{\infty} \langle d\rho_{el}/dz \rangle \exp(iq_z z)\, dz \right|^2 \qquad (A)$$

$$q_z = 4\pi\lambda^{-1}\sin\theta \qquad (B)$$

ideal forms of $\langle d\rho_{el}/dz \rangle$.

The first case is a single sharp interface located at $z = 0$. For such an interface, $\langle d\rho_{el}/dz \rangle$ takes the form of a delta function (eq C). The ρ_∞ in equation C is present as a

$$\langle d\rho_{el}/dz \rangle = \rho_\infty\, \delta(z) \qquad (C)$$

normalization factor. From the properties of the delta function,[2] equation A reduces to the expected Fresnel reflectivity, R_F (eq D).

$$R = R_F\, (\exp(iq_z 0))^2 = R_F\, (1)^2 = R_F \qquad (D)$$

We will now deduce the form of R for two sharp interfaces of equal height separated by a distance d. This situation is represented by two delta functions (eq E). Here

$$\langle d\rho_{el}/dz \rangle = 0.5\rho_\infty [\delta(z) + \delta(z-d)] \qquad (E)$$

the normalization factor is $0.5\rho_\infty$. Inserting this formula into equation A yields the form of R given by equation F.

$$R = (0.5)^2 R_F \left| \int[\delta(z) + \delta(z-d)]\exp(iq_z z)dz \right|^2$$

$$= 0.25 R_F \left| \int\delta(z)\exp(iq_z z)dz + \int\delta(z-d)\exp(iq_z z)dz \right|^2$$

$$= 0.25 R_F \left| 1 + \exp(iq_z d) \right|^2 \qquad (F)$$

We will consider the case of complete destructive interference (R = 0). Equation (F) then takes the form given by equation G. When we equate the real and complex parts of

$$0 = 1 + \exp(iq_z d) = 1 + \cos(q_z d) + i\sin(q_z d) \qquad (G)$$

both sides of equation G, we find that $q_z d$ must be an odd multiple of π (eq H). We now substitute for q_z from equation B (eq I). Rearrangement of equation I yields equation J

$$q_z d = (2n + 1)\pi \qquad n = \text{an integer} \qquad (H)$$

$$4\pi\sin\theta\, d\lambda^{-1} = (2n + 1)\pi \qquad (I)$$

$$2d\sin\theta = (2n + 1)\lambda/2 \qquad (J)$$

which is the usual condition for total destructive interference.[3] With a slightly more complex analysis we can

show that if the two sharp interfaces are of unequal height, equation J gives the angle at which the intensity of the reflected X-rays is at a minimum. If the two interfaces are not of the same height, however, the interference can never be totally destructive; that is, $R \neq 0$.

References

1. Als-Nielsen, J. Physica **1986**, 140A, 376-387.

2. Dirac, P. A. M. The Principles of Quantum Mechanics, 2nd ed.; Clarendon Press: Oxford, 1935; Chapter 4.

3. Halliday, D.; Resnick, R. Physics, 3rd ed., Part 2; John Wiley: New York, 1978; Section 45-5.

DL/1113/89/1

TECHNICAL REPORT DISTRIBUTION LIST, GENERAL

	No. Copies
Office of Naval Research Chemistry Division, Code 1113 800 North Quincy Street Arlington, VA 22217-5000	3
Commanding Officer Naval Weapons Support Center Attn: Dr. Bernard E. Douda Crane, IN 47522-5050	1
Dr. Richard W. Drisko Naval Civil Engineering Laboratory Code L52 Port Hueneme, California 93043	1
Defense Technical Information Center Building 5, Cameron Station Alexandria, Virginia 22314	2 high quality
David Taylor Research Center Dr. Eugene C. Fischer Annapolis, MD 21402-5067	1
Dr. James S. Murday Chemistry Division, Code 6100 Naval Research Laboratory Washington, D.C. 20375-5000	1
Dr. Ronald L. Atkins Chemistry Division (Code 385) Naval Weapons Center China Lake, CA 93555-6001	1
Chief of Naval Research Special Assistant for Marine Corps Matters Code 00MC 800 North Quincy Street Arlington, VA 22217-5000	1
Dr. Bernadette Eichinger Naval Ship Systems Engineering Station Code 053 Philadelphia Naval Base Philadelphia, PA 19112	1
Dr. Sachio Yamamoto Naval Ocean Systems Center Code 52 San Diego, CA 92152-5000	1
David Taylor Research Center Dr. Harold H. Singerman Annapolis, MD 21402-5067 ATTN: Code 283	1

POLYMER PROGRAM DISTRIBUTION LIST

Dr. J. M. Augl
Naval Surface Weapons Center
White Oak, MD 20910

Dr. A. S. Abhiraman
School of Chemical Engineering
Georgia Institute of Technology
Atlanta, GA 30332

4132033

Dr. Harry R. Allcock
Department of Chemistry
Pennsylvania State University
University Park, PA 16802

4132007

Dr. Chris W. Allen
Department of Chemistry
University of Vermont
Burlington, VT 05405

413c012

Dr. Ronald D. Archer
Department of Chemistry
University of Massachusetts
Amherst, MA 01003

413c028

Dr. Ali S. Argon
Mechanical Engineering Department
Massachusetts Institute of Technology
Cambridge, MA 02139

a400005df

Dr. William J. Bailey
Department of Chemistry
University of Maryland
College Park, MD 20742

413a006

Dr. Kurt Baum
Fluorochem, Inc.
680 S. Ayon Avenue
Azusa, CA 91702

4000021sbi

Dr. Frank D. Blum
Department of Chemistry
University of Missouri - Rolla
Rolla, MO 65401

413m005

Dr. Len J. Buckley
Naval Air Development Center
Code 6063
Warminster, PA 18974

Dr. F. James Boerio
Materials Science & Engineering Dept.
University of Cincinnati
Cincinnati, Ohio 45221

413m012

Dr. Ivan Caplan
DTNSRDC Annapolis
Code 0125
Annapolis, MD 21401

Dr. Robert E. Cohen
Department of Chemical Engineering
Massachusetts Institute of Technology
Cambridge, MA 02139

4132001

Dr. E. Fischer
DTNSRDC Code 2853
Annapolis, MD 21402

Dr. Curtis W. Frank
Department of Chemical Engineering
Stanford University
Stanford, CA 94305

413h005

Dr. Gregory S. Girolami
School of Chemical Sciences
University of Illinois
Urbana-Champagne, IL 61801

4132014

Dr. Robert H. Grubbs
Department of Chemistry
California Institute of Technology
Pasadena, CA 91124

4132019

Dr. James F. Haw
Department of Chemistry
Texas A&M University
College Station, TX 77843

413c039

Dr. Stuart L. Cooper
Department of Chemical Engineering
University of Wisconsin
Madison, WI 53706

4132006

Dr. Warren T. Ford
Department of Chemistry
Oklahoma State University
Stillwater, OK 74078

413h006

Dr. John K. Gillham
Department of Chemical Engineering
Princeton University
Princeton, New Jersey 08544

413c005

Dr. Bernard Gordon
Department of Polymer Science
Pennsylvania State University
University Park, PA 16802

413c025

Dr. Henry K. Hall
Department of Chemistry
University of Arizona
Tucson, AZ 85721

413j009

Dr. Alan J. Heeger
Department of Physics
University of California, Santa Barbara
Santa Barbara, CA 93106

4132012

Dr. Pat J. Hendra
Department of Chemistry
University of Southampton
Highfield Southampton 509 5NH
United Kingdom
4134001

Dr. Charles E. Hoyle
Department of Polymer Science
University of Southern Mississippi
Hattiesburg, MS 39406-0076

413c026

Dr. Bruce S. Hudson
Department of Chemistry
University of Oregon
Eugene, Oregon 97403

413c018

Dr. Leonard V. Interrante
Department of Chemistry
Rensselaer Polytechnic Institute
Troy, NY 12181

413c014

Dr. Hatsuo Ishida
Department of Macromolecular Science
Case Western Reserve University
Cleveland, OH 44106

413m008

Dr. Jeffrey T. Koberstein
Institute of Materials Science
University of Connecticut
Storrs, CT 06268

4132013

Dr. Paul M. Lahti
Department of Chemistry
University of Massachusetts
Amherst, MA 01003

413c037

Dr. Richard M. Laine
Washington Technology Center
University of Washington
Seattle, WA 98195

s400033srh

Dr. Robert W. Lenz
Polymer Science and Engineering Dept.
University of Massachusetts
Amherst, MA 01002

441c013

Dr. Geoffrey Lindsay
Chemistry Division - Code 087
Naval Weapons Center
China Lake, CA 93555

4132036

Dr. Alan D. MacDiarmid
Department of Chemistry
University of Pennsylvania
Philadelphia, PA 19104

a400004df

Dr. Chris W. Macosko
Materials Science & Engineering Dept.
University of Minnesota
Minneapolis, MN 55455

4132029

Dr. Joseph H. Magill
Materials Science & Engineering Dept.
University of Pittsburgh
Pittsburgh, PA 15161

413c013

Dr. Leo Mandelkern
Department of Chemistry
Florida State University
Tallahasee, FL 32306-3015

4132018

Dr. Tobin J. Marks
Department of Chemistry
Northwestern University
Evanston, IL 60201

413c030

Dr. Lon J. Mathias
Department of Polymer Science
University of Southern Mississippi
Hattiesburg, MS 30406-0076

413m003

Dr. Krzysztof Matyjaszewski
Department of Chemistry
Carnegie Mellon University
Pittsburgh, PA 15213

413j002

Dr. James E. McGrath
Department of Chemistry
Virginia Polytechnic Institute
Blacksburg, VA 24061

4132007

Dr. William B. Moniz
Code 6120
Naval Research Laboratory
Washington, DC 20375-5000

4132012

Dr. Kay L. Paciorek
Ultrasystems Defense and Space, Inc.
16775 Von Karman Avenue
Irvine, CA 92714

s400029srh

Dr. Virgil Percec
Department of Macromolecular Science
Case Western Reserve University
Cleveland, OH 44106-2699

413c024

Dr. Martin Pomerantz
Department of Chemistry
University of Texas at Arlington
Box 19065
Arlington, TX 76019-0065
a400008df

Dr. Roger S. Porter
Dept. of Polymer Science & Engineering
University of Massachusetts
Amherst, MA 01002

413m006

Dr. T. J. Reinhart, Jr.
Nonmetallic Materials Division
Air Force Materials Laboratory (AFSC)
Wright-Patterson AFB, OH 45433

Dr. Arnost Reiser
Insitute of Imaging Sciences
Polytechnic University
333 Jay Street
Brooklyn, NY 11021

4132022

Dr. Ferdinand Rodriguez
Department of Chemical Engineering
Cornell University
Ithaca, NY 14853

413c011

Dr. Charles M. Roland
Code 6120
Naval Research Laboratory
Washington, DC 20375-5000

413m009

Dr. Michael F. Rubner
Materials Science & Engineering Dept.
Massachusetts Institute of Technology
Cambridge, MA 02139

413m007

Dr. Ronald Salovey
Department of Chemical Engineering
University of Southern California
Los Angeles, CA 90089

413m010

Dr. Jacob Schaefer
Department of Chemistry
Washington University
St. Louis, MO 63130

413m001

Dr. Jerry I. Scheinbeim
Dept. of Mechanics & Materials Science
Rutgers University
Piscataway, NJ 08854

4132009

Dr. Lawrence R. Sita
Department of Chemistry
Carnegie Mellon University
Pittsburgh, PA 15213

4132030

Dr. L. E. Sloter
Code Air 931-A
Naval Air Systems Command
Washington, D. C. 20361-9310

Dr. Richard R. Schrock
Department of Chemistry
Massachusetts Institute of Technology
Cambridge, MA 02139

4132038

Dr. Dietmar Seyferth
Department of Chemistry
Massachusetts Institute of Technology
Cambridge, MA 02139

413c004

Dr. David S. Soane
Department of Chemical Engineering
University of California, Berkeley
Berkeley, CA 94720-9989

413h004

Dr. Les H. Sperling
Materials Research Center #32
Lehigh University
Bethlehem, PA 18015

413c002

Dr. Richard S. Stein
Polymer Research Institute
University of Massachusetts
Amherst, MA 01002

4132008

Dr. C. S. Sung
Institute of Materials Science
University of Connecticut
Storrs, CT 06268

413m011

Dr. Sukant K. Tripathy
Department of Chemistry
University of Lowell
Lowell, MA 01854

4132016

Dr. C. H. Wang
Department of Chemistry
University of Utah
Salt Lake City, Utah 84112

413c020

Dr. Kenneth B. Wagener
Department of Chemistry
University of Florida
Gainesville, FL 32611

a400007df

Dr. Robert A. Weiss
Department of Chemical Engineering
University of Connecticut
Storrs, CT 06268

a400006df

Dr. George M. Whitesides
Department of Chemistry
Harvard University
Cambridge, MA 02138

4132010

Dr. Garth L. Wilkes
Department of Chemical Engineering
Virginia Polytechnic Institute
Blacksburg, VA 24061

4132020